THE THERMODYNAMIC PRESSURE IN SUPERFLUID HELIUM AND ITS IMPLICATIONS FOR THE PHONON DISPERSION CURVE

By

ALBERT ROBERT MENARD III

A DISSERTATION PRESENTED TO THE GRADUATE COUNCIL
OF THE UNIVERSITY OF FLORIDA
IN PARTIAL FULFILLMENT OF THE REQUIREMENTS FOR THE
DEGREE OF DOCTOR OF PHILOSOPHY

UNIVERSITY OF FLORIDA

1974

To Anne, who made this possible

ACKNOWLEDGMENTS

The author would like to express his appreciation for help and guidance during the course of this work to the following persons:

Dr. E. D. Adams for suggesting this problem and providing aid in all phases of the research.

Dr. S. H. Castles for his frequent and timely advice.

Drs. L. H. Nosanow, J. S. Rosenshein and J. A. Titus for their encouragement and support.

Bill Steeger, the late Sherman Sharp, and the late George Harris for machining the many parts of the apparatus.

C. B. Britton, R. M. Mueller and B. Kummer for valuable assistance and suggestions.

Pat Coleman for producing the liquid helium used in the experiment.

Catherine Phillips for assistance in drawing the figures.

Margaret Anderson for an excellent job of typing under difficult circumstances.

TABLE OF CONTENTS

LIST OF TABLES

LIST OF FIGURES

Abstract of Dissertation Presented to the
Graduate Council of the University of Florida
in Partial Fulfillment of the Requirements for the
Degree of Doctor of Philosophy

THE THERMODYNAMIC PRESSURE OF SUPERFLUID HELIUM AND ITS IMPLICATIONS FOR THE PHONON DISPERSION CURVE

By

ALBERT ROBERT MENARD III

December 1974

Chairman: E. D. Adams
Major Department: Physics

The thermodynamic pressure of superfluid ^{4}He, for seven densities from near saturated vapor pressure to 11 atm., has been measured from 0.4 K to 1 K, using a capacitive strain gauge. A comparison of these measurements with calculations for the pressure, based on the phonon-roton model for superfluid helium, led to the conclusion that anomalous phonon dispersion exists in helium at low densities. The magnitude of the anomalous dispersion is in good agreement with that deduced from specific heat measurements. The conjecture of a quadratic term in the expression for the dispersion curve does not agree with these data. Contributions to the pressure not accounted for by phonons and rotons were observed. These contributions, probably maxons, increased in magnitude and became noticeable at a lower temperature as the density was increased.

CHAPTER I
INTRODUCTION

Historical Background

Liquid helium has been a source of fascination for physicists ever since helium gas was first liquified by Kammerlingh Onnes in 1908. The phase diagram of helium is shown in Fig. 1. Above the transition marked the λ line in Fig. 1, helium, usually referred to as He I, despite its obvious quantum properties, shows many of the thermodynamic and hydrodynamic properties characteristic of classical liquids. Below the transition, where it is referred to as He II, its characteristics undergo drastic qualitative changes and many of its properties are unique to helium. The most outstanding of these changes is that of superfluidity--the vanishing of flow resistance for the passage of the liquid through small channels. These properties are characteristic of natural helium, which is nearly 100% ^{4}He. The lighter isotope, ^{3}He, is present in natural helium in such small quantities (about one part in 10^6) that its effects are not noticeable in most experiments. The vast amount of theoretical and experimental work on liquid helium is well summarized by Wilks (1967), by Woods and Cowley (1973), and by Keller (1969).

The first major step toward a theory that would explain the unique properties of superfluid helium was the suggestion

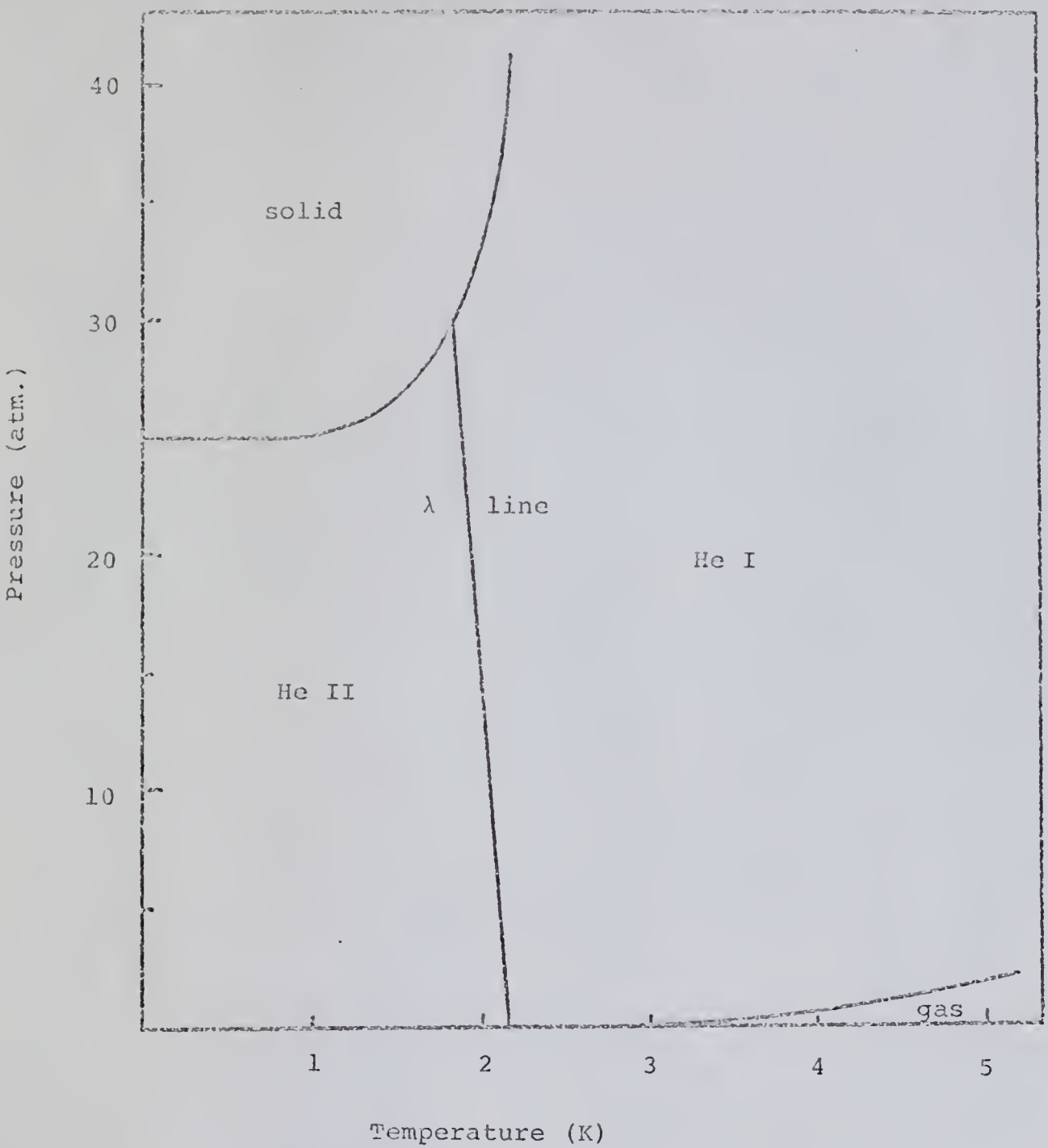

Fig. 1. Phase diagram of ^{4}He [after Wilks (1967)].

made by London (1954) that the superfluid phase was a "fourth state of matter" representing a macroscopic manifestation of quantum effects. He reasoned that a significant fraction of the liquid, or perhaps the whole liquid, might exist in a single quantum state. Because ^{4}He has zero spin, it will obey Bose-Einstein statistics: in contrast, the rare isotope ^{3}He which has spin 1/2 will obey Fermi-Dirac statistics. In Bose statistics an unlimited number of particles may occupy an energy level. This has the mathematical consequence that an ideal gas of bosons, i.e., a large number of non-interacting particles subject to Bose statistics, will for certain values of the density and temperature of the gas have a significant fraction of the particles "condensed" into the ground state. This "condensation" will occur in momentum space. Thus particles separated by large distances in the fluid will have their momenta, hence their motion, correlated. Fermi statistics do not permit this unless there is a pairing of the atoms. Thus the experimental fact that ^{3}He is not a superfluid until less than 0.003 K, in contrast to 2.17 K for the superfluid transition in ^{4}He, is easily explained.

This suggestion by London and Tisza provided the basis for the development of a two-fluid model. London (1954) gives a full account of the historic development of this idea and the role played by Tisza in its development. Helium was viewed as being composed of two interpenetrating fluids--a superfluid with zero entropy and a normal fluid. The two-fluid model successfully predicted most of the macroscopic

thermal phenomena in ^{4}He. It also explained the tremendous differences in low temperature properties between ^{3}He and ^{4}He. However, this model had four grave weaknesses. (1) It was a macroscopic and not a microscopic theory. (2) The agreement between theory and experiment was qualitative, not quantitative. (3) The theory was difficult to extend to dynamical situations such as the propagation of sound. (4) Finally, the theory was a model, many of whose features, such as the existence of the condensate, could not be experimentally verified.

The next major advance was the Landau (1941, 1947) theory of superfluidity. Landau viewed superfluid helium as a perfect background fluid in which a gas of elementary excitations moves. These excitations, which have a definite energy and momentum, describe the "collective motion" of the helium atoms similarly to the use of "normal modes" to describe the motion of interacting particles. The excitations behave as quasi-particles which interact very weakly with each other. From the energy spectrum, i.e., the relation between energy and momentum for the excitations, thermodynamic and hydrodynamic properties of liquid helium can be deduced. The excitations were given the names "phonons" and "rotons."

Landau pictured the phonon excitations as long wavelength density fluctuations with energy, ε, directly proportional to their momentum, p, and traveling with the velocity of sound, c. Thus,

$$\varepsilon = cp \qquad (1.1)$$

in the long wavelength limit. At shorter wavelengths (larger p) the ε versus p dispersion curve passes through a minimum, such that

$$\varepsilon = \Delta + (p - p_o)^2/2\mu. \qquad (1.2)$$

The excitations in the region of the minimum were called rotons. While the excitation spectrum is a smooth, continuous curve, at low temperatures only the phonon and roton states are significantly populated. Since the excitations were associated with the "normal" fluid and the background was identified with the superfluid, most of the results of the two-fluid model could be derived from Landau's theory. However, there was still no physical microscopic basis, nor was there an experimental basis, for the assumptions of the theory, and the experimentally verified necessity that superfluid helium be a Bose system had vanished from the theory. If a microscopic physical basis for the energy spectrum of the excitations could be provided, the Landau theory would provide an adequate description for almost all phenomena in helium.

Feynman (1953, 1954) showed that a liquid consisting of indistinguishable particles subject to Bose statistics could have only one kind of low energy excitations. These were density fluctuations resembling sound waves which when quantized were identical with Landau's phonons. Since Feynman's

arguments were very general, based on the energy of a configuration of individual atoms, this provided a microscopic explanation for the phonon part of the excitation spectrum. In a further paper, relying again on very generalized arguments, Feynman (1954b) calculated a wave function for liquid helium which included the possibility of rotational motion. By applying the variational principle, the energy spectrum was found to be

$$\varepsilon(p) = \frac{p^2}{2m} S(k) \tag{1.3}$$

where $S(k)$ is the liquid structure factor. For the small k limit at $T = 0$ this reduces to $\varepsilon(p) = cp$. At higher momentum, the structure factor, which can be measured by X-ray scattering from the fluid, has a maximum which leads to a minimum in $\varepsilon(p)$. The resulting spectrum is in qualitative agreement with Landau's proposal. An improved wave function due to Feynman and Cohen (1956) greatly improved the agreement between the computed energy spectrum and the Landau type spectrum as determined from thermodynamic measurements. Finally, Feynman and Cohen (1957) pointed out that the excitations could be observed directly by neutron scattering. Neutron scattering experiments, discussed in the next section, confirmed the excitation picture by directly measuring the excitations and showed that their spectrum had the form suggested by Landau. Thus the theory had a firm physical

basis and the condition that the particles obey Bose statistics was automatically included in the theory.

However, this was still not a "first principles" calculation. There have been numerous attempts to derive the spectrum from a consideration of the interaction potential for two helium atoms and the application of statistical mechanics. Despite considerable formal progress, the microscopic theory has not yet been developed sufficiently to give a detailed description of liquid helium. However, considerable progress has been made in variational calculations for the structure factor and the ground state energy, for example, Pokrant (1972). A comprehensive summary of these efforts and their shortcomings can be found in Keller (1969) and in Woods and Cowley (1972).

Neutron and X-ray Scattering Measurements

After Feynman's paper, several groups performed neutron scattering experiments. The most comprehensive of the early works was that of Yarnell *et al.* (1959). This work measured an excitation spectrum that was in good agreement with the one proposed by Landau based on thermodynamic arguments. Also it showed that below 1.5 K the line width of the excitations was quite narrow. This implied that the excitations had a relatively long lifetime and that the interactions between excitations were weak, two critical assumptions of the theory. As the temperature approached the λ line, the excitations became very broad and strongly interacting and

changed character for temperatures above the λ line, thus confirming that the measured spectrum was connected with superfluidity, since the superfluid properties become less pronounced near the λ line and vanish above it.

With improvements in technique and technology, more work followed, culminating in the "definitive work" by Cowley and Woods (CW, 1971), whose work was accurate enough to permit attempts to fit the spectrum with algebraic expressions. Recently Dietrich *et al.* (1972) undertook a comprehensive study of the roton dip in the spectrum, including a study of its variation with pressure. Three major problems have occurred in all neutron scattering measurements. Neutron scattering is limited to values of k greater than about 0.4 A^{-1}, and the measurements for small k values have a very large intrinsic error. Except for the roton work of Dietrich *et al.* and some work at 24 atm. by Svensson, Woods and Martel (1972), and Henshaw and Woods (1961), there has been no work on the pressure variation of the excitation spectrum. Finally, all neutron measurements have been taken above 1.1 K, so there is a question of possible variation of the curves with temperature below that point. Nevertheless neutron scattering is the most direct and most accurate way of measuring the excitation spectrum.

In addition to direct measurement of the excitation spectrum, neutron scattering, as well as X-ray scattering, can be used to measure the structure function, $S(k,\omega)$. The structure factor relates the differential coherent scattering cross section to the total cross section

$$\frac{d^2\sigma}{d\Omega dE} = \frac{\sigma}{4\pi\hbar} \frac{k'}{k_o} S(k,\omega) \qquad (1.4)$$

where $d\Omega$ is the solid angle of acceptance of the scattered beam, dE is the energy width of the scattered beam, k_o and k' are, respectively, the incident and scattered wave numbers, σ is the total cross section and $\hbar\omega$ is the energy transfer during the scattering. Since S depends on the momentum transfer during the scattering process, frequently $S(k,\omega)$ is written $S(Q,\omega)$ where Q is a new variable defined as the momentum transfer. Because the Fourier transform of S is the time dependent correlation function, S is related to the spatial and temporal behavior of the atoms in the fluid.

As shown by Eq. (1.3), the structure factor can be related to the excitation spectrum. There is reasonable agreement between the spectrum obtained directly from neutron scattering and that deduced indirectly from the structure factor as obtained in the best recent measurements of Hallock (1972). As with the neutron scattering measurements of the excitation spectrum, structure factor measurements are limited to k greater than 0.33 A^{-1}. There has been essentially no work on the pressure dependence of S. Hallock did carry the measurements down to 0.38 K, which, while it is not T = 0 as used in most theories, does eliminate most questions about temperature variation. Scattering can also be used to hunt directly for the presence of the condensate, but results so far are inconclusive because of serious experimental

problems--for a review of the subject see Jackson (1974). Thus scattering measurements have thoroughly demonstrated the "reality" of Landau's excitations and have provided a quantitative basis for the theory which is in good numerical agreement with the values deduced from thermodynamic measurements, but there are still gaps in the measured spectrum, particularly in the long wavelength-small p region.

By fitting the experimental scattering data with the assumed form given by Eqns. (1.1) and (1.2), explicit values for μ, Δ, p_0 and c can be obtained. These values can then be used in a statistical mechanical analysis to yield expressions for the pressure, specific heat, entropy, expansion coefficient and the superfluid density used in the two-fluid model. This will be done explicitly in Chapter II. These expressions can be compared directly with experimental values. Historically, the process was reversed, with values for μ, Δ, p_0 and c being deduced from thermodynamic measurements and these values were used to construct the excitation spectrum. In general there is good agreement between calculated and measured thermodynamic properties. This agreement is usually expressed by comparing the values of μ, p_0, Δ and c derived from scattering with those derived from thermodynamics. There is a major flaw in this scheme: since thermodynamic measurements simultaneously sample the entire excitation spectrum, any deviation of the spectrum from the assumed forms can lead to a change in the parameters. This is a particularly severe problem with rotons, since the

measured excitation spectrum is not parabolic except in a very narrow region around the minimum. Most of the difference between the thermodynamic values for μ, Δ, p_0 and c, and the neutron values of μ, Δ, p_0 and c can be accounted for by this problem. Thus the phonon-roton picture of liquid helium rests on a sound phenomenological basis--neutron scattering--and successfully predicts most of the thermodynamic properties of helium.

Measurements of the Velocity and Attenuation of Sound

Only one parameter in the phonon-roton model can be directly measured other than by scattering. That parameter is c, the sound velocity. Many measurements of the sound velocity and the attenuation of sound have been made. The most comprehensive of these was a series of measurements made at the Argonne Laboratories, Abraham *et al.* (1969, 1970) and Roach *et al.* (1972a, 1972b), which measured sound velocity, attenuation of sound, and the Gruniessen constant, $\Gamma = \frac{\rho}{c}\frac{\partial c}{\partial \rho}$ (where ρ is the density), as a function of pressure, frequency and temperature in the region below 0.6 K. These measurements could be compared with the detailed predictions, for these quantities in liquid helium, developed by Khalatnikov and co-workers--Andreev and Khalatnikov (1963), Khalatnikov (1965), and Khalatnikov and Chernikova (1965, 1966). Their results were based on the development of quantum hydrodynamics for superfluid helium by Landau and Khalatnikov as

summarized by Khalatnikov (1965). For there to be attenuation of sound, Eq. (1.1) was modified to

$$\varepsilon = cp(1 - \gamma p^2). \tag{1.5}$$

Some modification was necessary, since a pure phonon spectrum, $\varepsilon = cp$, does not permit phonon decay because of the impossibility of simultaneously satisfying energy and momentum conservation except through the quantum mechanical uncertainty of ε. Experimentally the energy width is known to be far too small to permit the observed attenuation. The additional term containing γ is known as dispersion. The exact form of the dispersion term was a reasonable assumption, but was not the only possibility. Since Landau and Khalatnikov's theory had been successful in predicting most hydrodynamic phenomena in liquid helium, it was a major surprise when their predictions were qualitatively wrong about the measured values of the velocity and attenuation of sound as well as their variation with temperature, pressure, and frequency at very low temperatures. The theoretical prediction for the attenuation, α, was that in low temperature limit α would be proportional to T^6. The experimental result was that α was proportional to T^4. Furthermore the measured attenuation was approximately two times greater than the calculated attenuation. As the pressure was raised, a strange "shoulder" appeared in the data although nothing of the sort had been predicted. The velocity of sound showed extremely complicated behavior as a function of frequency and

temperature which had not been predicted. As Abraham *et al.* (1969) remarked, "We therefore conclude that the present theoretical formulation of sound propagation at very low temperatures is incomplete" (p. 370). How could a model which had so successfully predicted so many of the properties of helium fail so miserably in the low temperature limit where it should perform the best?

Recent Theoretical Developments

Although substantially confirmed by neutron scattering, the phonon-roton picture of helium, like the two-fluid model, is a model. Keller's (1969) warning about models is appropriate. "A model is devised to represent a physical phenomenon because the actual situation is far too complicated to be handled directly; the model then incorporates the simplifying assumptions that make the problem tractable. The first danger is one of oversimplification, and this is an especially hazardous possibility when quantum effects are involved ....

When such a [good] model exists, there is a tendency to take it too literally, to promote it to too high a status, and then finally to forget it is a model" (p. 17). One such oversimplification of the phonon-roton model can be seen in Fig. 2. Clearly phonons and rotons are a very poor approximation to the actual excitation spectrum in the region of the maximum of the curve and on the high k side of the minimum. To check the possibility that this oversimplification might affect calculations based on the model, Bendt *et al.* (1959)

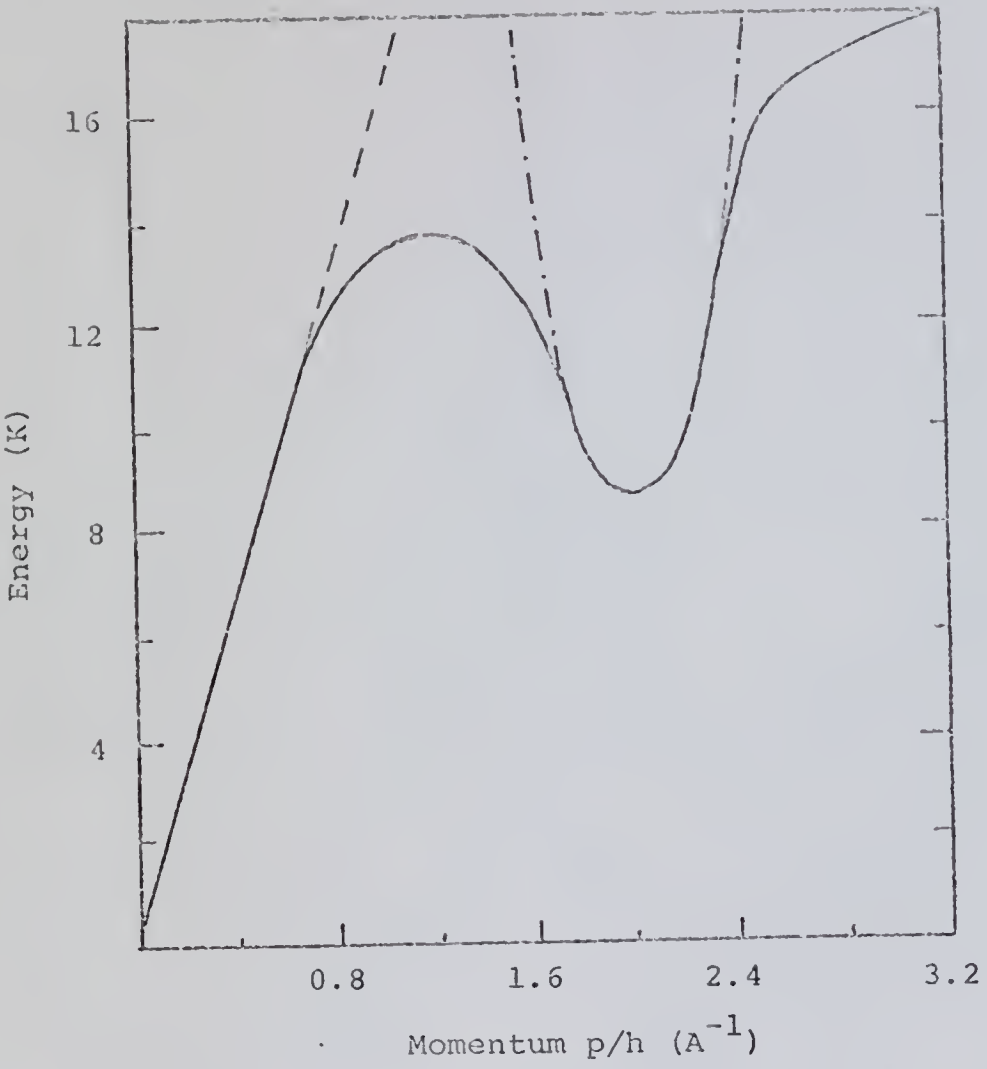

Fig. 2. Excitation spectrum at SVP [after Cowley and Woods].

dashed line is the phonon approximation, dashed and dotted line is the roton approximation.

and Singh (1968) made the laborious and complex calculations of some of the thermodynamic properties of liquid helium directly from the measured excitation spectrum. They found that calculations based on the phonon-roton model deviate very little from their exact calculations at low temperatures, but that these deviations increase sharply with increasing temperature, becoming quite large above 1.5 K. Because the whole model collapses rapidly as one approaches the λ transition, this is not surprising. Unfortunately, no work has ever been done on the pressure dependance of the deviations of the phonon-roton model from exact calculations, partly because no extensive neutron scattering studies have been done as a function of pressure. Only very high precision measurements of thermodynamic properties will show deviations from the phonon-roton model since the total deviation is of the order of 2% for temperatures near 1 K and decreases rapidly as the temperature is lowered below 1 K.

There would appear to be little possibility that there is any major flaw in the theory of sound propagation, since it has worked so well for other materials. Thus attention focused on the approximation that $\varepsilon(p) = cp(1 - \gamma p^2)$. If, as Landau had assumed, γ was greater than 0, then the dispersion was normal, i.e., the type found in most materials. Normal dispersion prohibits three-phonon processes by the conservation laws. Three-phonon processes are those where one phonon decays into two others, or where two phonons combine to make a third. All theorists agree that the only way to produce

the experimentally observed T^4 dependence of the attenuation of sound at low temperatures is by allowing three-phonon processes to occur.

Simon (1963) and Petick and Ter Haar (1966) showed that, under some circumstances, three-phonon processes were allowed without dispersion. Due to the finite lifetime of the phonons, the phonon spectrum has a width which allows the conservation equations to be satisfied. However, Friedlander, Eckstein and Kuyper (1972) claimed to have shown that proper renormalization of phonons forbids three-phonon processes for all cases of "normal" dispersion. The best fit to the CW rerults at saturated vapor pressure was the phonon spectrum $\varepsilon = cp(1 - \gamma p^2 - \delta p^4)$ with $\gamma = 0 \pm 2 \times 10^{36}$ and $\delta = 2.4 \pm .3 \times 10^{75}$. This disagreed sharply with $\gamma = 8 \times 10^{37}$ derived from ultrasonic measurements by Eckstein and Varga (1968) using Khalatnikov's approach. Havlin and Luban (1972) were able to fit the ultrasonic data with a spectrum $\varepsilon(p) = cp(1 - \delta p^4)$; but their $\delta \sim 0.9 \times 10^{75}$ was a factor of 3 lower than the neutron value. As will be shown in detail in Chapter II, no thermodynamic measurement can separate the effect of γ^2 from the effect of δ. So, unless γ remains very small over a considerable range of pressure, an analysis based solely on δ has limited usefulness. The high pressure neutron measurements of Svensson, Woods and Martel, which had $\gamma = 6.2 \pm 0.6 \times 10^{37}$, argued against any assumption that γ was insignificantly small over the entire pressure range of liquid helium.

Maris and Massey (1970) suggested that if γ were less than zero--so-called anomalous dispersion--the problems of the theory would be solved. Anomalous dispersion unquestionably permits three-phonon processes. Further calculations by Maris (1972, 1973), in which he solved the integral equations for velocity and attenuation of sound numerically without the customary approximations, but assumed anomalous dispersion, were in good agreement with the experimental data on attenuation and velocity of sound below about 14 atm. pressure. These calculations yielded a value of -8×10^{37} for γ at saturated vapor pressure.

Jackle and Kehr (1971) were able to explain the shoulder in the attenuation data by using anomalous dispersion and introducing a cutoff frequency. The cutoff occurred because of an assumption that an ultrasonic phonon, i.e., one produced by the experimenter, could only be absorbed by a thermal phonon, i.e., one already present in the liquid due to its finite temperature, if the thermal phonon had a momentum $\hbar k$ less than $\hbar k_c$. This reproduced the shoulder very well if k_c was a strong function of pressure, decreasing sharply with increasing pressure. That implied that the shape of the phonon spectrum was very sensitive to pressure. Using available data on the shape of the curve, they predicted that the effect of the cutoff would be most noticeable between 14 and 19 atm., in accord with experiment.

The assumption that γ is negative would radically change the generally accepted ideas about phonon-phonon interactions.

While agreement with the ultrasonic data was gratifying, at that time there was little other experimental evidence to support this assumption. There were hints from the neutron data that this might be possible, since earlier neutron work by Henshaw and Woods (1961) had reported the possibility that γ was negative. There was also evidence from X-ray scattering that the small k structure factor was not inconsistent with a negative γ. This result was given a boost with a model calculation by Iachello and Rassetti (1973), based on a new technique of deriving the spectra from the helium potential curve, yielded a model which had anomalous dispersion at low pressures and normal dispersion at higher pressures. Also Zasada and Pathria (1972) had shown a similar result; negative γ at low densities, positive γ at higher densities could be obtained for an imperfect Bose gas by using reasonable potentials. Experimental evidence discussed in the next subsection has tended to support this hypothesis.

A recent calculation by Jackle and Kehr (1974) concluded, on the basis of ultrasonic measurements at finite temperatures, that γ was negative and nearly constant with pressure, while δ was positive and increased rapidly with pressure. Thus the apparent normal dispersion at higher pressures would be caused by δ becoming so large as to dominate γ rather than by γ changing signs.

All of the preceding calculations have assumed that the phonon spectrum is given by

$$\varepsilon(p) = cp(1 - \gamma p^2 - \delta p^4 \ldots). \tag{1.6}$$

The series is assumed to terminate with the δ term in the sense that higher order terms are too small to be observed. Feenberg (1971) showed that for a simple interatomic potential, such as the inverse r^6, e.g., the dipole-dipole potential, that $S(p)$ and $\varepsilon(p)$ must contain both even and odd powers of p beyond the cubic term. Thus there was no a priori reason why the expansion for $\varepsilon(p)$ should not include all powers of p. This suggestion led Molinari and Regge (MR, 1971) to reanalyze the results of CW yielding a five-term fit

$$\varepsilon(p) = c\hbar p(1 + 0.5465p - 1.3529p^2 + 0.2595p^3 + 0.1860p^4 - 0.0522p^5)^{1/2} \tag{1.7}$$

with both even and odd powers. Most experimental evidence seems to indicate that the coefficient of the p^2 term of the expansion is zero. This destroys the ability of the formula to fit the neutron data.

At about the same time, Gould and Wong (1971) showed that for a weakly interacting Bose gas there are terms of the form $p^5 \log(1/p)$ in both $\varepsilon(p)$ and $S(p)$. Their fairly general arguments indicated that, to the extent that helium could be treated as a weakly interacting Bose gas, no analytic expansion of $\varepsilon(p)$ was possible. However, since their complete spectrum was of the form $\varepsilon(p) = c_o p + c_2 p^3 + c_L p^5 \log(1/p)$ it would be difficult to detect the non-polynomial terms. The source of the singularity lay in the multiphonon interactions.

While multiphonon interactions are important in helium, it is very questionable whether a weakly interacting Bose gas is a good model for multiphonon interactions in helium. So far, no one has analyzed the experimental data to look for evidence of the predicted log (1/p) term, due to the formidable mathematical difficulties in doing such an analysis.

Lin-Liu and Woo (1974) presented a calculation based on sum rules which the structure should obey. This yielded a phonon spectrum at P = 0 and T = 0 of the form

$$\varepsilon(p) = cp\left(1 + 0.17 \left(\frac{p}{mc}\right)^2 + 0.78 \left(\frac{p}{mc}\right)^3 - 3.3 \left(\frac{p}{mc}\right)^4\right). \qquad (1.8)$$

The positive numbers indicate anomalous dispersion. In this calculation, the anomalous dispersion comes from both the p^3 term--the term with coefficient γ in the usual expansion--and the p^4 term. The p^5 term--the term with coefficient δ in the usual expansion--has normal dispersion. No comments were made about the pressure dependence of any of the coefficients. With the exception of the work of Jackle and Kehr (1974), all calculations of the spectra are for T = 0 at zero applied pressure. With the exception of MR, all of the formulas for the excitation spectrum are in agreement with experimental data. This is hardly surprising since most experiments can just barely detect the effect of the γp^2 term, making positive identification of the higher order terms difficult and the assignment of accurate numerical values virtually impossible.

Recent Experimental Results

The principal experimental evidence has been a set of specific heat measurements by Phillips, Waterfield and Hoffer (PWH, 1970). They measured the specific heat of liquid helium at four different pressures. At low pressures they found evidence for anomalous dispersion. If $\varepsilon = cp(1 - \gamma p^2)$, then $\gamma = -4.1 \times 10^{37}$ at saturated vapor pressure. γ decreased in magnitude with increasing pressure and became positive somewhere between 5 and 20 atm. At 20 atm., they found $\gamma = +19.6 \times 10^{37}$. They claimed their work could also be fitted, though "less well" at saturated vapor pressure by $\gamma = 0$ and $\delta = -4.5 \times 10^{76}$. No other fits were attempted. There is some question about the validity of the analysis performed on the specific heat data by PWH. Nevertheless, the data are so significant that most theories are tested by reanalyzing these data to see if they can be fitted by the theory. No other thermodynamic data accurate enough to be analyzed have been published.

A recent reanalysis of these specific heat data by Zasada and Pathria (1974), using the measured neutron spectra instead of the phonon-roton approximation, yielded $\gamma = -5.1 \times 10^{37}$ at saturated vapor pressure. Similar analysis was performed on the data at the other two "low pressures," changing γ slightly, but no fit was attempted for the highest pressure.

Similarly the X-ray measurements of S(p) of Hallock (1972) could be analyzed to give $\gamma = -5.7 \times 10^{37}$. However,

they could also be analyzed to yield a quadratic term as proposed by MR or to give a $\gamma = -3 \times 10^{36}$, i.e., = 0 to within the quoted error of CW.

Since the quadratic term $\alpha_1 p^2$, proposed by MR, was of lower order than the usual γp^3 term, there were immediate attempts to observe it. Anderson and Sabisky (1972) measured the acoustic thickness of helium films at 1.38 K for frequencies between 20 and 60 GHz. Their analysis yielded a positive quadratic term in good agreement with MR. These frequencies were over an order of magniture greater than the usual ultrasonic frequencies, the largest of which was 256 MHz. The temperature was also much higher than usual, since most measurement of phonon properties are made below 0.6 K. Recently Anderson and Sabisky (1974) stated that their analysis of film properties may have been inadequate.

Roach *et al.* (1972c) measured the frequence dependence of the sound velocity with an improved technique at T = 0.3 K at frequency 30 and 90 MHz. They reported that if $\varepsilon(p) = cp(1 + \alpha_1 p)$, then $\alpha_1 = 0 \pm 0.01$ A, in sharp contrast to $\alpha_1 = 0.275 \pm 0.030$ A for Anderson and Sabisky (1972) and MR. A reanalysis of the specific heat data by Zasada and Pathria (1972) concluded that the inclusion of a quadratic term in the energy spectrum led to a set of parameters whose behavior as a function of density was too erratic to be acceptable; whereas, setting α_1 identically equal to zero led to a set of parameters which, as a function of density, were in agreement with direct measurements of the same quantities. This

experimental evidence is generally regarded as showing that there is no quadratic term in the excitation spectrum.

The uncertainties in the experimental situation are illustrated by two recent experiments. (1) Narayanamurti, Andres and Dynes (1973) measured the group velocity and attenuation of phonons with frequencies of 2×10^{10} to 9×10^{10} Hz, far in excess of any ultrasonic measurements. They report zero dispersion over the whole range of frequencies. As noted by Jackle and Kehr (1974), there appear to be some inconsistencies in the analysis of Narayanamurti *et al.* For example, in 1974 Dynes and Narayanamurti used three-phonon processes to analyze their experiments with heat pulses in helium. The phonon lifetimes used in the heat pulse analysis are inconsistent with three-phonon processes occurring in the absence of dispersion. The heat pulse experiments did show a striking change near 15 to 17 atm. and normal dispersion at higher pressures. (2) Mills *et al.* (1974) measured the angular spreading of phonon beams, which they interpreted to be evidence for negative (anomalous) dispersion below 17 atm. and normal dispersion above that. This analysis was based on the presence or absence of three-phonon processes as shown by the width of a phonon beam.

In summary, the weight of the evidence suggests that there is anomalous dispersion in liquid helium at low pressures and normal dispersion at higher pressures. However, more high precision experimental data are needed to decide

among the different theories. This thesis was undertaken to provide high precision measurements of the thermodynamic pressure as a function of both density and temperature below 1 K. The results will be compared with the predictions of the different theories. The measurements were also carried to higher temperatures to compare them with the measurements of pressure as a function of density and temperature above 1.5 K made by Keesom and Keesom in 1933.

CHAPTER II
LANDAU THEORY

Algebraic Results

In this chapter the predictions of the thermodynamic pressure for the different phonon spectra will be computed. If one adopts the Landau model for helium, then the thermodynamic properties of liquid helium are determined by the excitations. If there are $N_{\underset{\sim}{p}}$ excitations with momentum $\underset{\sim}{p}$ and energy $\varepsilon(\underset{\sim}{p})$, the total energy of the fluid is

$$E\{N_{\underset{\sim}{p}}\} = E_o + \sum_{\underset{\sim}{p}} N_{\underset{\sim}{p}}\, \varepsilon(\underset{\sim}{p}) \tag{2.1}$$

where E_o is the ground state energy. This is the fundamental assumption of Landau--all of the energy of the system can be accounted for by the excitations of the single particle excitation spectrum $\varepsilon(\underset{\sim}{p})$. However, this is not strictly true. As CW showed, there are other branches of the excitation spectrum. However, these lie at such high energy, ε/k greater than 18 K, that they should have little effect on low temperature (less than 1 K) properties, due to the weighting factor $\exp(-\varepsilon/kT)$ in thermodynamic calculations.

By definition, the partition function for a liquid is

$$Z = Z_o \sum_{\{N_{\underset{\sim}{p}}\}} \exp(-\beta E\{N_{\underset{\sim}{p}}\}) \tag{2.2}$$

where β has its usual definition, $\beta = 1/kT$. Assuming that the excitations are bosons, which would be expected for a system of Bose particles, this equation reduces to

$$Z = Z_o \prod_{\underset{\sim}{p}} [1-\exp(-\beta\varepsilon(\underset{\sim}{p}))]^{-1} \tag{2.3}$$

The Helmholtz free energy is defined to be $F = -kT \log Z$. Thus, F is given by

$$F = -kT \sum_{\underset{\sim}{p}} \log[1-\exp(-\beta\varepsilon(\underset{\sim}{p}))]^{-1} + F_o \tag{2.4}$$

where $F_o = -kT \log Z_o$ is the ground state free energy. Assuming a continuum distribution of states so that $\sum_{\underset{\sim}{p}} = \frac{V}{h^3} \int d^3\underset{\sim}{p}$, then

$$F = -\frac{kTV}{h^3} \int \log[1-\exp(-\beta\varepsilon(\underset{\sim}{p}))]^{-1} d^3\underset{\sim}{p} + F_o \tag{2.5}$$

This result assumes, in agreement with experimental results, that $\varepsilon(p)$ is a smooth, well-behaved function. For a fluid one can assume isotropy, i.e., properties of the material depend only on the magnitude of $\underset{\sim}{p}$, not its direction. Thus one can replace $d^3\underset{\sim}{p}$ by $4\pi p^2 dp$, yielding

$$F = F_o + \frac{4\pi kTV}{h^3} \int_o^\infty \log[1-\exp(-\beta\varepsilon(p))] p^2 dp. \tag{2.6}$$

Integrating by parts gives

$$F = F_o - \frac{4\pi kTV}{3h^3} \int_o^\infty \frac{p^3 \, d[\beta\varepsilon(p)]}{\exp(\beta\varepsilon(p))-1}. \tag{2.7}$$

This assumes that $\lim_{p\to\infty}\varepsilon(p) = \infty$, which is true for all physical systems.

In addition to the mathematical approximations discussed above, there are two assumptions inherent in this approach which must have their validity checked. (1) The excitations are well-defined, long-lived and weakly interacting so that they can be treated as independent entities. This is confirmed by neutron measurements. (2) The excitation spectrum is a fixed quantity, neither varying with temperature for a fixed density nor varying rapidly with small density changes. To be useful, the spectrum must not vary during an experiment. For example, it will be assumed that the spectrum is constant in this experiment, although the temperature varies from 0.3 K to 0.9 K. Since neutron scattering measurements extend only to 1.1 K, this assumption cannot be experimentally proven for temperatures less than 1 K. However, neutron measurements are almost independent of temperature between 1 K and 1.5 K. Similarly, the sound velocity, which is an explicit parameter in the excitation spectrum, varies by less than 0.1% for temperatures between 0.1 K and 1 K and varies slowly with density. However, theoretical calculations by Ishikawa and Yamada (1972) showed that for an imperfect Bose gas the higher order terms, such as γp^2, varied considerably with temperature and that temperature variations in the interactions between excitations would have the same effect as introducing new higher order terms. Because these variations only become large for temperatures greater than 1

K, the rest of this development of the theory will assume that the excitation spectrum is fixed in temperature.

Knowing $\varepsilon(p)$ from neutron and X-ray scattering, and more indirect sources, one calculates F from Eqns. (2.6) or (2.7). Then, the thermodynamic functions P, S, E, and C_V are calculated by the usual formulas:

$$P = -\left(\frac{\partial F}{\partial V}\right)_T, \quad S = -\left(\frac{\partial F}{\partial T}\right)_V, \quad E = F + TS, \quad C_V = \left(\frac{\partial E}{\partial T}\right)_V.$$

In practice, the calculation of F is very difficult unless further approximations are made. Furthermore, the calculation of the thermodynamic functions is extremely difficult unless F is known as an algebraic function of temperature, T, and volume, V.

The usual approximation for helium at saturated vapor pressure is shown by the dotted lines in Fig. 2. Fig. 3 shows the actual excitation spectrum and the phonon-roton approximation for helium at 24 atm. pressure. Separate free energies are computed for the phonons and rotons. Thus, $F = F_o + F_r + F_{ph}$. F_o, the free energy at 0 K, is independent of temperature. The volume derivative of F_o gives P_o, the pressure at 0 K. P_o will be treated as an experimental parameter and will not be calculated. To calculate F_r one inserts the roton spectrum $\varepsilon(p) = \Delta + (p-p_o)^2/2\mu$ into Eq. (2.6). Only a very small error is introduced by extending the limits of integration to 0 and ∞. Since the energy gap, Δ, is large compared to the temperature, the logarithm can be expanded to

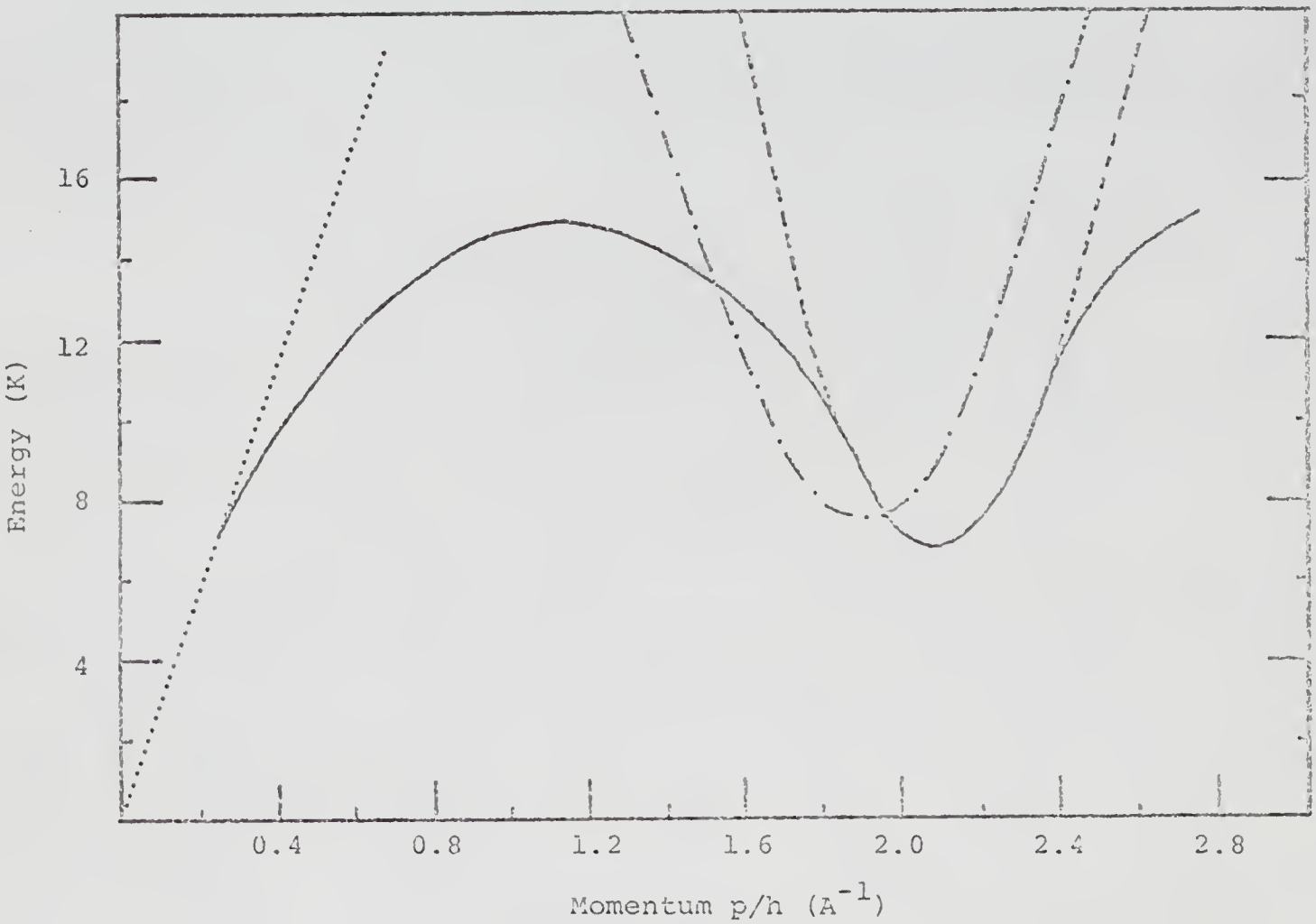

Fig. 3. Excitation spectrum at 24 atm.

dotted line is the phonon approximation, dashed and dotted line is the roton approximation calculated from Mills (1965), dashed line is the roton approximation calculated from Donnelly (1972).

first order, i.e., $\log [1-\exp(-\beta\varepsilon(p)) \simeq \exp(-\beta\varepsilon(p))]$. Because of the exponential weighting factor and the relatively small width of the minimum, the major contribution to the integral will come from $p \sim p_o$, so that the p^2 in the integrand of Eq. (2.6) may be replaced by p_o^2. This gives

$$F_r = -\frac{4\pi kTV}{h^3} \exp(-\Delta/kT) p_o^2 \int_0^\infty \exp(-(p-p_o)^2/2\mu kT)dp. \qquad (2.8)$$

Integrating gives the result

$$F_r = -(2(\mu kT)^{1/2} p_o^2 kTV \exp(-\Delta/kT))/((2\pi)^{3/2}\hbar^3). \qquad (2.9)$$

This yields

$$P_r = \frac{-\partial F_r}{\partial V} = 2(\mu kT)^{1/2} p^2 kTV \exp(-\Delta/kT) \qquad (2.10)$$
$$[1 + \frac{\Delta}{kT}\frac{\rho}{\Delta}\frac{\partial\Delta}{\partial\rho} - 1/2\ \frac{\rho}{\mu}\frac{\partial\mu}{\partial\rho} - \frac{2\rho}{p_o}\frac{\partial p_o}{\partial\rho}]/((2\pi)^{3/2}\hbar^3)$$

In order to compute the pressure in a useful form, the variation of Δ, p_o and μ with density must be known. Donnelly (1972) calculated the following values for the Landau parameters as a function of density. For ρ in gm/cm^3, these values are

$$\begin{aligned} \Delta/k &= (16.99 - 57.31\rho) \text{ Kelvin} \\ p_o/\hbar &= 3.64\rho^{1/3} \text{ inverse Angstroms} \\ \mu &= (0.32 - 1.103\rho)M_{^4He} \text{ grams} \end{aligned} \qquad (2.11)$$

These simple algebraic forms, based on the neutron scattering work of Dietrich *et al.* (1972) will be used in preference to

the graphical tables of Mills (1965), which were based on thermodynamic data. At low pressure the two different methods yield similar values for Δ, p_o and μ, but have substantially different values for the density derivatives $\frac{\partial \Delta}{\partial \rho}$, $\frac{\partial p_o}{\partial \rho}$, and $\frac{\partial \mu}{\partial \rho}$. At higher pressures, the two approaches disagree about both the values of the Landau parameters and the values of their density derivatives. The differences between the Mills and the Donnelly roton spectra can be seen in Fig. 3. Measurements of S_r by van den Meijdenberg *et al.* (1961) yield Landau parameters in substantial agreement with Donnelly if the corrections at low pressures suggested by van den Meijdenberg *et al.* are applied to their results. Using Donnelly's values for Δ, p_o and μ and their variation with density, one obtains

$$P_r = \frac{2kT}{(2\pi)^{3/2}\hbar}\{[kT(0.32 - 1.103\rho)]^{1/2}\ [3.64\rho^{1/3}]^2 \qquad (2.12)$$

$$[1/3 - \frac{57.31\rho}{T} + \frac{.5515\rho}{0.32 - 1.103\rho}]\ [\exp((57.31\rho - 16.99)/T)]\}$$

F_{ph} is calculated in a similar fashion. A phonon spectrum, the most general form encompassing all proposed formulas except that of Gould and Wong,

$$\varepsilon(p) = cp(1 + \alpha_1 p + \alpha_2 p^2 + \alpha_3 p^3 + \alpha_4 p^4 \ldots)$$

is inserted in Eq. (2.7). The limits of integration are extended to infinity. This causes complete overlap of the integrals for F_r and F_{ph}. However, the resulting error is

small because of the large values of ε_r and ε_{ph} in the regions of overlap. This yields

$$F_{ph} = -\frac{\pi V(2\pi k)^4}{180h^3c^3}\left[T^4 - \frac{45\alpha_1 B(5)}{2\pi^5}\left(\frac{2\pi k}{c}\right)T^5 + \frac{10}{7}(3\alpha_1^2-\alpha_2)\left(\frac{2\pi k}{c}\right)^2 T^6\right.$$

$$+ \frac{15B(7)}{8\pi^7}(15\alpha_1\alpha_2 - 3\alpha_3 - 16\alpha_1^3)\left(\frac{2\pi k}{c}\right)^3 T^7$$

$$+ 1/2(54\alpha_1^4 + 12\alpha_2^2 - 75\alpha_1^2 + 18\alpha_1\alpha_3 - 3\alpha_4)$$

$$\left.\left(\frac{2\pi k}{c}\right)^4 T^8\right] \qquad (2.13)$$

where B(n) equals the Gamma function of n times Zeta function of n. Hence, the pressure is

$$P_{ph} = \frac{\pi(2\pi k)^4}{180h^3c^3}\left\{(1+3\Gamma)T^4 - \frac{45B(5)}{2\pi^5}\left(\frac{2\pi k}{c}\right)\left[(1+4\Gamma)\alpha_1 - \rho\frac{\partial\alpha_1}{\partial\rho}\right]T^5\right.$$

$$+ 10/7\left(\frac{2\pi k}{c}\right)^2\left[(1+5\Gamma)(3\alpha_1^2-\alpha_2) - \rho\left(6\alpha_1\frac{\partial\alpha_1}{\partial\rho} - \frac{\partial\alpha_2}{\partial\rho}\right)\right]T^6$$

$$+ \frac{15}{8\pi^7}B(7)\left(\frac{2\pi k}{c}\right)^3\left[(1+6\Gamma)(15\alpha_1\alpha_2 - 3\alpha_3 - 16\alpha_1^3)\right.$$

$$\left.- \rho\left(15\alpha_1\frac{\partial\alpha_2}{\partial\rho} + 15\alpha_2\frac{\partial\alpha_1}{\partial\rho} - 3\frac{\partial\alpha_3}{\partial\rho} - 48\alpha_1^2\frac{\partial\alpha_1}{\partial\rho}\right)\right]T^7$$

$$+ 1/2\left(\frac{2\pi k}{c}\right)^4\left[(1+7\Gamma)(54\alpha_1^4 + 12\alpha_2^2 - 75\alpha_1^2\alpha_2 + 18\alpha_1\alpha_3 - 3\alpha_4)\right.$$

$$- \rho\left(216\alpha_1^3\frac{\partial\alpha_1}{\partial\rho} + 24\alpha_2\frac{\partial\alpha_2}{\partial\rho} - 150\alpha_1\alpha_2\frac{\partial\alpha_1}{\partial\rho} - 75\alpha_1^2\frac{\partial\alpha_2}{\partial\rho}\right.$$

$$\left.\left.\left.+ 18\alpha_1\frac{\partial\alpha_3}{\partial\rho} + 18\alpha_3\frac{\partial\alpha_1}{\partial\rho} - 3\frac{\partial\alpha_4}{\partial\rho}\right)\right]T^8\right\} \qquad (2.14)$$

where $\Gamma = \frac{\rho}{c}\frac{\partial c}{\partial \rho}$ is the Gruniessen constant. This expression is the first four terms of the MR formula. The standard form for most theories is $\varepsilon(p) = cp(1 - \gamma p^2 - \delta p^4)$, i.e., $\alpha_1 = \alpha_3 = 0$, $\alpha_2 = -\gamma$ and $\alpha_4 = -\delta$. For this case Eq. (2.13) becomes

$$F_{ph} = -\frac{\pi V(2\pi k)^4}{180h^3c^3}\left[T^4 + \frac{10}{7}\gamma\left(\frac{2\pi k}{c}\right)^2 T^6 + 1/2(12\gamma^2 + 3\delta)\left(\frac{2\pi k}{c}\right)^4 T^8\right] \tag{2.15}$$

and Eq. (2.14) reduces to

$$P_{ph} = \frac{\pi(2\pi k)^4}{180h^3c^3}\left\{(1 + 3\Gamma)T^4 + \frac{10}{7}\left(\frac{2\pi k}{c}\right)^2\left[(1 + 5\Gamma)\gamma - \rho\frac{\partial\gamma}{\partial\rho}\right]T^6 + 3/2\left(\frac{2\pi k}{c}\right)^4\left[(1 + 7\Gamma)(4\gamma^2 + \delta) - \rho\left(8\gamma\frac{\partial\gamma}{\partial\rho} + \frac{\partial\delta}{\partial\rho}\right)\right]T^8\right\} \tag{2.16}$$

As a check on the validity of these calculations for pressure, E, C_v and S were calculated from the free energy--Eqns. (2.9) and (2.15). These expressions for E, C_v and S were compared with other calculations of those quantities by Zasada and Pathria (1972), Roach *et al.* (1972e) and Donnelly (1967) and were found to be in exact agreement. These calculations led to the discovery that Eq. (2) in PWH (p. 1260) is incorrect. The correct form is

$$C_V = \frac{\pi V(2\pi k)^4}{15h^3c^3}\left[T^3 + \frac{25}{7}\left(\frac{2\pi k}{c}\right)^2\gamma T^5 + 7(4\gamma^2 + \delta)\left(\frac{2\pi k}{c}\right)^4 T^7 \ldots\right]$$

Numerical Results

The first term in Eq. (2.16), $\pi(2\pi k)^4(1+3\Gamma)T^4/180h^3c^3$, common to all theories, will be referred to as the phonon pressure. Similarly, Eq. (2.12) gives the roton pressure. To compute the magnitude of the pressure due to the dispersion term in the phonon spectrum, one needs the values of γ and $\partial\gamma/\partial\rho$. Table I gives the values of γ and $\partial\gamma/\partial\rho$ for three phonon spectra derived from experimental results. The values of γ and $\partial\gamma/\partial\rho$ for most of the theories of superfluid helium fall within the range of values of these three spectra. The value of $\partial\gamma/\partial\rho$ is calculated by assuming a linear variation of γ with ρ, i.e., $\partial\gamma/\partial\rho = (\gamma_{24\ \text{atm.}} - \gamma_{SVP})/(\rho_{24\ \text{atm.}} - \rho_{SVP})$.

Because this thesis concerns the measurement of pressure, numerical estimates of the size of the various contributions to the pressure are necessary. Table II gives numerical values of the phonon pressure, roton pressure, and the pressure due to dispersion for each of the spectra in Table I. These values are given at saturated vapor pressure and at 24 atm.--the two extremes of pressure accessible in the liquid. Values for both 1 K and 0.5 K are given since the upper limit of validity for the approximation that there are only phonons and rotons present is 1 K, and since the effects of dispersion are clearest near 0.5 K. For all of the spectra except MR the dispersion pressure varies as T^6. For MR the dispersion pressure varies as T^5, which should make MR readily distinguishable from the other spectra, although the absence of any comment by MR on the variation of their spectrum with

Table I. Values of the Dispersion Parameter, γ, and Its Density Derivative in c.g.s. Units, Based on Experimental Data

Method	SVP	24 Atmospheres	$\frac{\partial \gamma}{\partial \rho}$
Ultrasonic	8×10^{37} [a]	6×10^{37} [b,d]	-7.3×10^{38}
Neutron	0 [c]	6×10^{37} [d]	2.19×10^{39}
Specific Heat	-4.1×10^{37} [e]	19.6×10^{37} [e]	8.65×10^{39}

[a]Eckstein and Varga (1968)

[b]Mills *et al.* (1974), Svensson, Woods and Martel (1972)

[c]Cowley and Woods (1971)

[d]Svensson, Woods and Martel (1972)

[e]Phillips, Waterfield and Hoffer (1970)

Table II. Contributions of Different Terms to the Pressure, Expressed in Atmospheres, at Saturated Vapor Pressure and at 24 Atmospheres

Term	0.5 K	1.0 K
Phonon		
SVP	1.47×10^{-3}	2.35×10^{-2}
24 atm.	3.33×10^{-4}	5.34×10^{-3}
Roton		
SVP	-1.18×10^{-6}	-9.29×10^{-3}
24 atm.	-3.29×10^{-5}	-5.33×10^{-2}
Phonon plus Roton		
SVP	1.47×10^{-3}	1.42×10^{-2}
24 atm.	3.04×10^{-4}	-4.79×10^{-2}
Dispersion		
Ultrasonic		
SVP	9.71×10^{-5}	6.21×10^{-3}
24 atm.	9.74×10^{-6}	6.23×10^{-4}
Neutron		
SVP	-2.27×10^{-5}	-1.48×10^{-3}
24 atm.	3.07×10^{-6}	1.96×10^{-4}
Specific Heat		
SVP	-1.37×10^{-4}	-8.78×10^{-3}
24 atm.	7.7×10^{-6}	4.94×10^{-4}

density makes it impossible to calculate a value for the dispersion pressure for their phonon spectrum. The values of pressure in Table II should be compared with P_o, which ranges from approximately 0.1 atm. for an all-liquid sample just above saturated vapor pressure to approximately 24 atm. for an all-liquid sample just below the melting curve.

It is difficult to calculate the T^8 term in Eq. (2.16)--the next order correction term--since it depends on γ^2, $\gamma\ \partial\gamma/\partial\rho$, δ, and $\partial\delta/\partial\rho$. To estimate the size of the T^8 term at 1 K, γ and $\partial\gamma/\partial\rho$ were taken from PWH. δ was set equal to $4\gamma^2$ and $\partial\delta/\partial\rho$ was set equal to $8\gamma\ \partial\delta/\partial\rho$, so that the contribution of δ, and $\partial\delta/\partial\rho$ to the T^8 pressure term would be equal to the contribution of γ and $\partial\gamma/\partial\rho$. This gave a value of $\delta = 10^{76}$ and $\partial\delta/\partial\rho = -2 \times 10^{78}$ at saturated vapor pressure. Only Jacklc and Kehr (1974) have a δ greater than 10^{76} at saturated vapor pressure. However, the large positive variation of their δ with ρ would tend to cancel the effect of the large δ term. Despite this maximization of the T^8 term, it is less than 10% of the T^6 term at 1 K and decreases more rapidly with decreasing temperature than the T^6 term.

It is also necessary to estimate the error caused by the inaccuracy of the phonon-roton approximation in the region of the maximum of the excitation spectrum, shown in Figs. 2 and 3. If one introduces another type of excitation, called maxons, characterized by an equation of the form

$$\varepsilon(p) = \Delta' - \frac{(p - p_o')^2}{2\mu'}$$

over a restricted range, the properties of the superfluid can be analyzed in terms of three excitations instead of two. Unfortunately, because of the necessity of restricting the range of integration on each of the excitations, the integrals in Eqns. (2.7) and (2.8) can no longer be done in closed form. They must be done numerically. Since the spectrum for the maxons is similar to the roton spectrum, the equation for pressure will be similar to Eq. (2.10). Thus the maxon pressure will vary as $\exp(-\Delta'/kT)$. Substituting a reasonable Δ' in Eq. (2.11) gives a pressure equal to approximately 5% of the roton pressure for low pressures. Since the roton pressure is considerably smaller than the phonon pressure, the effect of the maxons is negligible for temperatures below 1 K. As shown by Fig. 3, at higher pressures the situation is different, the height of the maxons changes only slightly, but the width approximately triples. Because Δ' increases, the pressure due to the maxons will be positive. A reasonable estimate is that the contribution of the maxons will be approximately 10% of the roton pressure at higher density. Because the roton pressure is equal to or larger than the phonon pressure at these densities, this will introduce a serious error. From Fig. 3 it would appear that the Mills spectrum, derived from thermodynamic measurements, is shifted to lower p, higher Δ, and broader μ in order to average in the effects of the maxons. Thus the difference between the thermodynamic values for μ, p_o and Δ and the neutron

values at high densities may be due to the inadequacy of the phonon-roton approximation in the region of the maximum of the spectrum. If the maxons produce a pressure large enough to interfere with measurements at higher densities, one could use the Mills roton spectrum to alleviate the problem.

From Table II it is evident that one needs a pressure resolution of the order of 10^{-5} atm. at saturated vapor pressure to clearly see the dispersion pressure. At 24 atm. a resolution of the order of 10^{-6} atm. is required, which implies a substantially higher instrumental resolution. If such resolution could be obtained, pressure measurements would differentiate between the different predictions of the dispersion parameters.

CHAPTER III
EXPERIMENTAL APPARATUS AND PROCEDURE

The Cryogenics

The cryostat is similar to the one described by Walsh (1963). It has been substantially modified from the one described by Heberlein (1969). The main features of the cryostat are a helium bath, a vacuum space, a ^{4}He refrigerator, a ^{3}He refrigerator and a sample chamber. Fig. 4 shows the cryostat schematically.

The vacuum space is enclosed by a copper cylindrical container which is attached to a flange on the cryostat. The vacuum-tight seal is made with 0.075 cm diameter pure indium wire. The vacuum space surrounds the ^{4}He refrigerator, the ^{3}He refrigerator and the sample chamber. When the apparatus is first being cooled down, by filling the helium bath, the vacuum space is filled with helium gas for purposes of thermal contact. It is then evacuated by pumping for several hours with a Consolidated Vacuum Corporation PMCS-2C oil diffusion pump backed by a Welch model 1400 pump. To prevent contamination there is a nitrogen trap in the pumping line.

The ^{4}He refrigerator has an internal volume of approximately 250 cm^3. It is filled from the bath via a modified Hoke valve operated by a long shaft extending through the top flange of the cryostat. This refrigerator can be maintained

Fig. 4. Schematic drawing of the cryostat.

A Electrical feed-throughs

B Pumping line for vacuum space

C Diffusion pump for ^{3}He refrigerator

D Mechanical pump for ^{3}He refrigerator

E Trap for ^{3}He return line

F Vacuum space flange

G ^{4}He refrigerator

H ^{3}He refrigerator

I Low temperature valve

J Radiation shield

K Sample chamber

L Vacuum can

M Pumping line for ^{4}He refrigerator

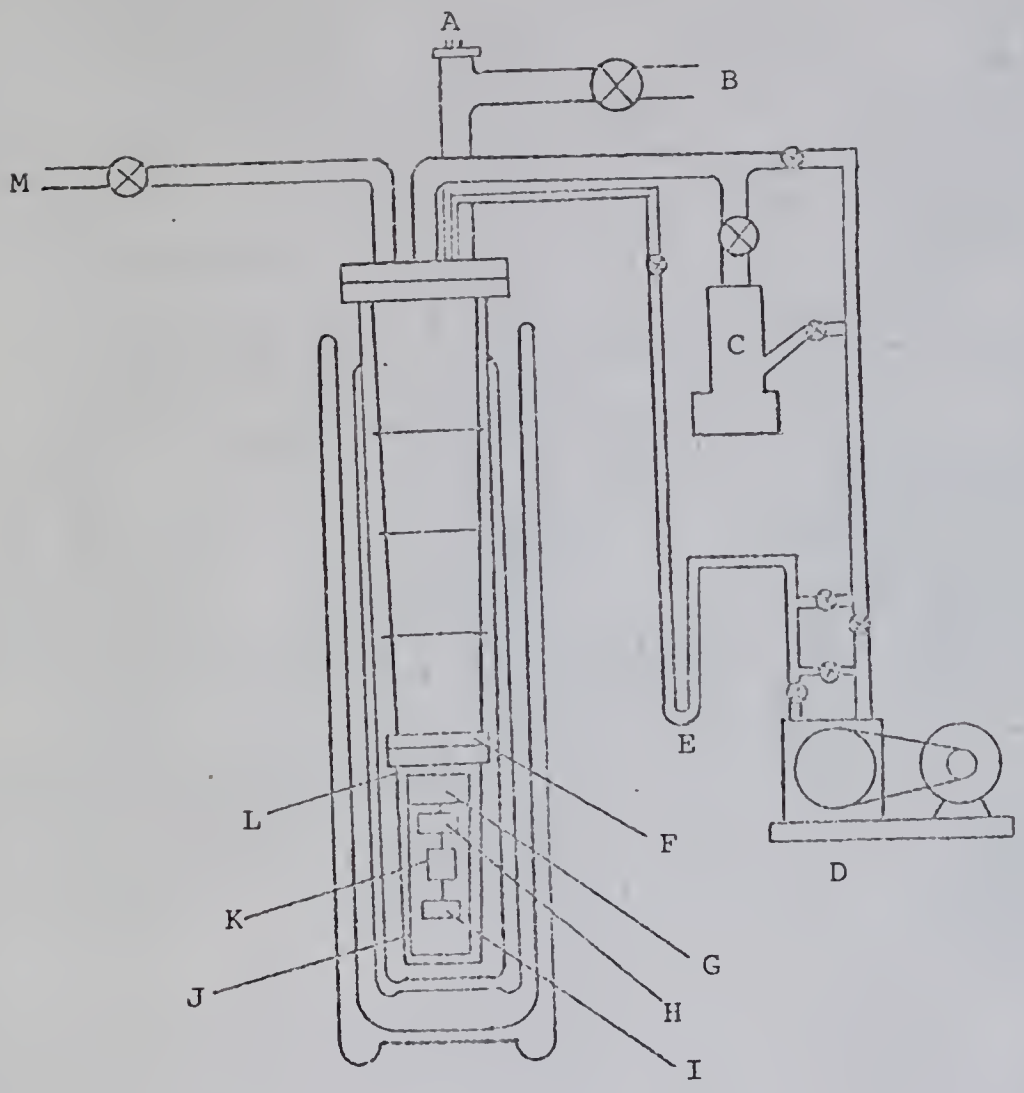
A
B
M
C
E
D
L
F
K
G
J
H
I

at a temperature of approximately 1.2 K for over 24 hours by pumping on the enclosed helium with a Kinney model KC-46 pump.

A radiation shield, attached to the underside of the ^{4}He refrigerator, surrounds the ^{3}He refrigerator and the sample chamber. The shield was constructed in the following manner. A mat of #44 bare copper wire was wound on a drum. A coat of General Electric 7031 varnish was applied to hold the mat together. The mat was then fitted around and epoxied onto a thin phenolic plastic form. The upper ends of the copper wires were stripped of varnish and soldered onto a copper ring which screwed into another copper ring bolted to the bottom of the ^{4}He refrigerator. This arrangement provided the largest possible cross-sectional area for experimentation below the ^{4}He refrigerator.

The ^{3}He refrigerator was designed for continuous operation. The refrigerator holds approximately 1 cm^3 of liquid ^{3}He. To increase thermal contact between the ^{3}He and a copper flange, which is the base of the ^{3}He refrigerator, approximately 1 meter of thin (0.025 cm) copper foil was placed in the refrigerator and hard soldered to the base. The returning ^{3}He gas is forced to pass through a trap immersed in liquid nitrogen. This trap consisted of several layers of copper wire mesh followed by Linde molecular sieve #13 X. To provide the pressure drop needed to liquefy the returning ^{3}He gas, an impedance was placed in the return line below the ^{4}He refrigerator. The impedance was made by

inserting approximately 18 cm of 9 mil copper wire into a 10-mil-i.d. copper-nickel capillary. A National Research Corporation model B-2 oil diffusion pump backed by a Welch model 1402 pump with an oil shaft seal for closed system operation was capable of reducing the temperature of the sample chamber to about 0.45 K. By closing a value on the ^{3}He return line and operating for periods up to two hours in the "single shot" mode, colder temperatures--about 0.39 K for the sample chamber--were achieved.

The sample chamber is supported by a 15 cm long, pitch bonded graphite rod approximately 1 cm in diameter. To provide thermal contact between the ^{3}He refrigerator and the sample chamber, a copper rod with a diameter of 0.5 cm was screwed into the base of the ^{3}He refrigerator and a length of copper braid with a diameter of 0.4 cm was hard soldered into a copper rod which screwed into the sample chamber. The two copper pieces were connected by a lead heat switch. The heat switch was 0.30 cm wide by 1 cm long by 0.03 cm thick. It was joined to the copper pieces with a thin coat of soft solder. Around the switch was placed a small, 1 cm bore, superconducting solenoid capable of generating a field of 1000 gauss with a current of 3 amps. The solenoid was powered by a 6 volt battery which also provided the current for the heater on the persistent switch.

The Sample Chamber and Pressure Measurement

The sample chamber shown in Fig. 5 was a modification of the capacitive strain gauge described by Straty and Adams

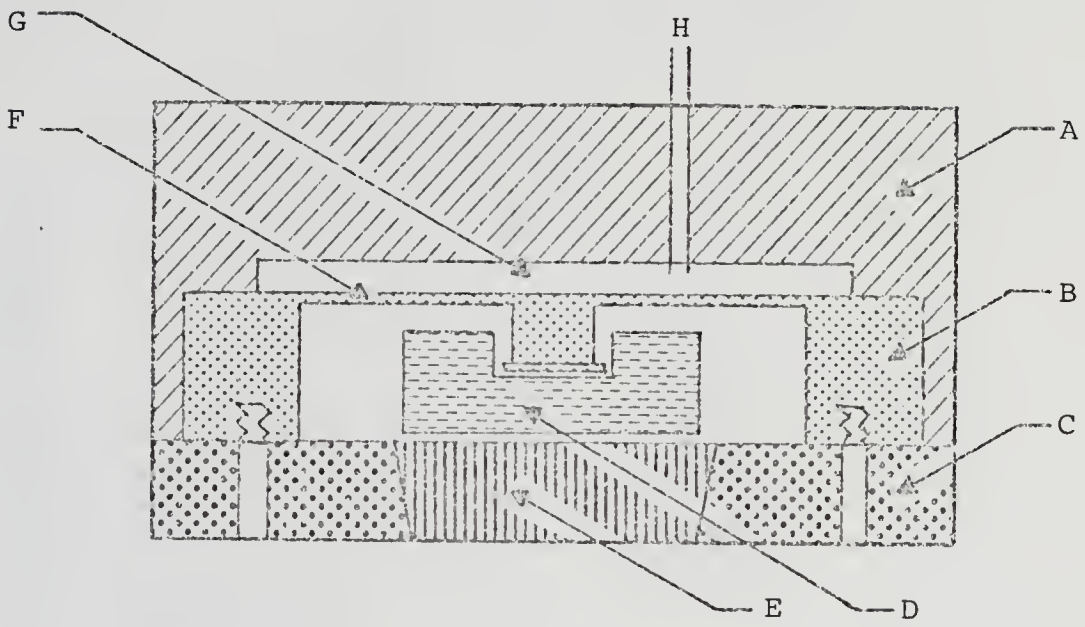

Fig. 5. Sample chamber

A Body of the chamber

B Diaphragm support

C Guard ring

D Moveable capacitor plate

E Fixed capacitor plate

F Diaphragm

G Sample

H Inlet Capillary

The copper brush is not shown

(SA, 1969). The cell had a volume of approximately 5 cm^3 and a height of 0.42 cm. To increase thermal contact to the sample, the interior of the cell was filled with fine copper wires using the technique of Kirk, Castles and Adams (1971). These wires had a surface area of approximately 250 cm^2 and filled about 30% of the volume of the cell. The main body of the cell was made of copper, while the diaphragm and the capacitor plates were made of berylium copper. The diaphragm was 0.2 cm thick. The upper capacitor plate was epoxied onto a post machined into the center of the diaphragm, so that as the diaphragm flexed the upper plate moved. The lower capacitor plate was held in a fixed position by a guard ring bolted to the piece containing the diaphragm.

Changes in the sample pressure cause a deflection of the diaphragm, which produces a change in the capacitance by changing the spacing between the capacitor plates. Expanding Eq. (7) in SA, one can show that

$$P - P_o \simeq A(C - C_o) + B(C - C_o)^2 + D(C - C_o)^3 + E(C - C_o)^4 + \ldots, \qquad (3.1)$$

where P is pressure and C is capacitance. In practice, the coefficients D and E are so small that the contribution of those terms is negligible except for very large pressures. Because of the very small spacing of the plates, 0.0012 to 0.0025 cm, any imperfections in the plates will cause shorting at low pressure. The plates were reasonably free of

imperfections, since a pressure of about 15 atm. was reached before shorting. In order to reach higher pressure, the plate spacing was increased to 0.0075 cm. With this spacing, the plates remained unshorted to a pressure of over 30 atm.

The capacitance was measured with a General Radio type 1620 A capacitance bridge. An Ithaco model 391 A lock-in was used to detect the balance of the bridge. A General Radio 1321 A audio oscillator provided a 10 v, 500 Hz signal to drive the bridge. With this arrangement, changes in capacitance as small as 10^{-5} pF could easily be detected. This corresponds to a pressure change of from 1×10^{-6} atm. to 5×10^{-6} atm., depending on the pressure. As the pressure increases, the sensitivity increases because the plates are closer together. Thus this apparatus could easily detect the dispersion pressure.

The capacitance was measured by a three-terminal technique which uses a separate coaxial line for each plate with neither plate grounded. This prevented shifts in capacitance due to small movements of the leads. To reduce any effect of changing temperature on the bridge, it was placed in a large, insulated box. The temperature of the laboratory was regulated so that the largest temperature drift over the course of a run was 1° F. The measured drift rate of the bridge never exceeded 2×10^{-5} pF for 8 hours.

The calibration of the strain gauge consisted of observing the capacitance of the gauge versus the pressure read on a gauge in the external system. The external gauge was a

Heise model #7770--a dial type Bourdon Gauge. Calibration of the strain gauge extended over a wide range of pressures--from 0 to 10 or 14 atm. The calibration points, consisting of a capacitance and a corresponding pressure, were used to find the coefficients of Eq. (3.1) by means of a least squares program. For this calibration P_o was 0 and C_o was the capacitance of the cell at 4 K when evacuated. The resulting fit had an RMS deviation of less than 0.01 atm. The absolute accuracy of the calibration measurements was no better than 0.05 atm., the absolute accuracy of the gauge. However, the relative accuracy, i.e., the accuracy in the measurement of small changes in pressure at a given pressure, was much higher being limited by the resolution of the strain gauge and the accuracy of the derivative dP/dC. The values of dP/dC must be fairly accurate to obtain a good fit over a wide range. The thermodynamic pressure is the pressure at constant volume. Obviously, the volume of the cell is not strictly constant. SA, in Eq. (8), show that

$$\left(\frac{\partial P}{\partial T}\right)_V = \frac{dP}{dT}\left(1 + \frac{1}{k_T V}\frac{dV}{dP}\right) \qquad (3.2)$$

where k_T is the isothermal compressibility of the sample. For this apparatus the correction term is less than 0.5%. Furthermore, Boghosian and Meyer (1966) showed that k_T is virtually independent of temperature below 1 K, varying by less than 0.01%, and that k_T varies very slowly with pressure. The geometrical factor $\frac{1}{V}\frac{dV}{dP}$ is independent of temperature and pressure below 1 K for small pressure changes. As

shown in Table II, the total variation in pressure between 0 and 1 K is approximately 10^{-2} atm. Such pressure changes have negligible effect on k_T and $\frac{1}{V}\frac{dV}{dP}$. Thus the correction for the change in volume of the cell is constant with temperature below 1 K. The analysis of the data will be concerned mainly with the temperature dependence of the pressure, so a small--less than 0.5%--constant correction should not affect the analysis of the data. For that reason the correction will be ignored in subsequent analysis.

Since the thermodynamic pressure is the pressure at constant volume and constant density, it is necessary to isolate the cell from the external pressure system. At first a valve on top of the cryostat was used. This proved unsatisfactory because of variations in the pressure in the filling capillary. These variations were caused by the normal changes in the level of the liquid helium bath which changed thermal gradients in the filling capillary even though it was inside an evacuated tube. To alleviate this problem a low temperature valve, shown in Fig. 6, based on the design of Roach *et al.* (1972d) was built. The valve was mounted immediately below the sample chamber so that the valve was at the same temperature as the sample cell. The valve seal was made by a Teflon-tipped brass stem sealing against a brass seat. The end of the brass stem was threaded and then machined to a conical shape. The inside of the Teflon tip was machined to the same geometry and screwed onto the brass stem. In this way, the Teflon tip was fully supported by metal. The valve

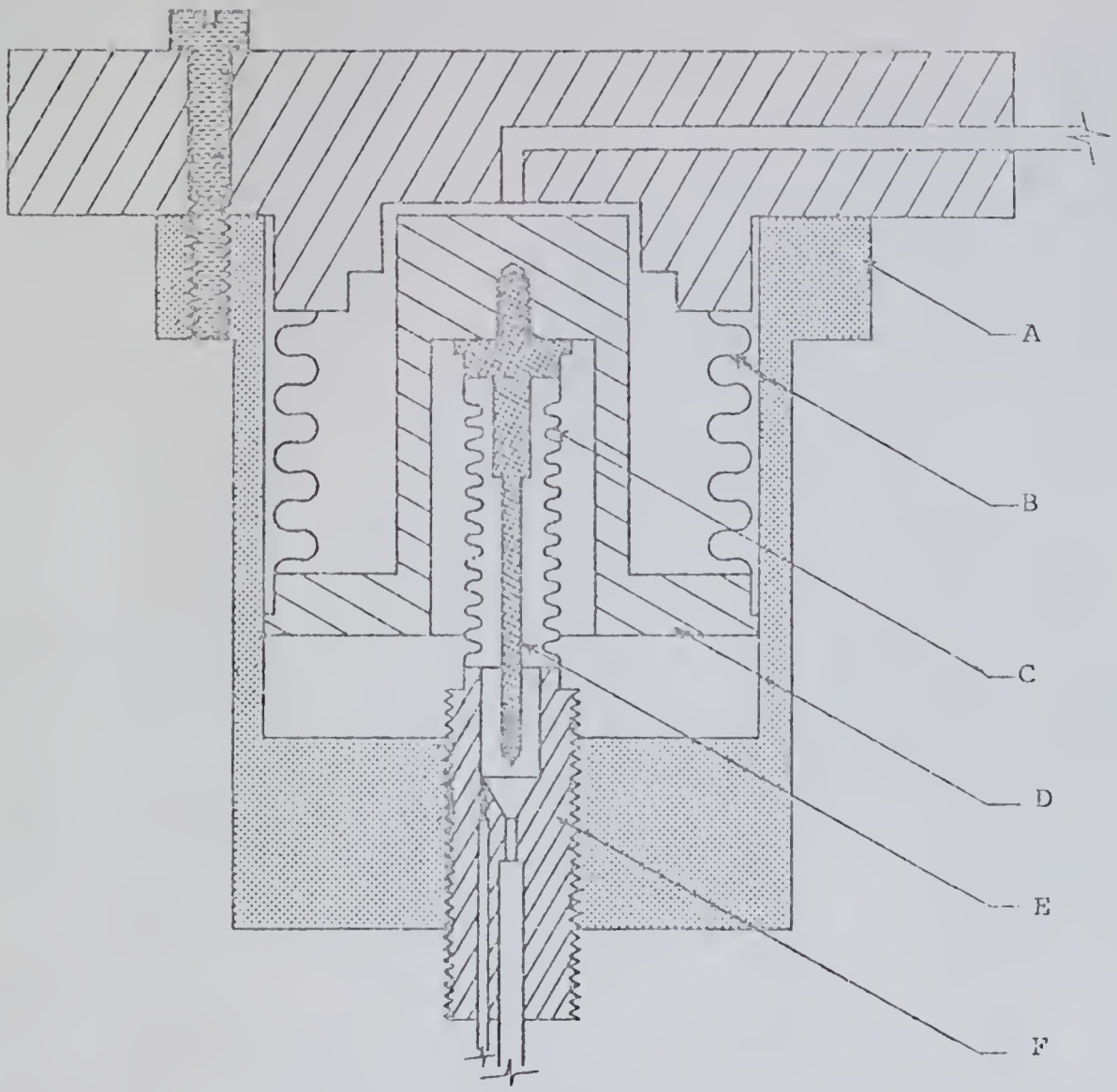

Fig. 6. Schematic diagram of low temperature valve.

A Valve body

B Accuator bellows

C Valve bellows

D Accuator piston

E Valve stem

F Valve seat

was an hydraulic one, operated by changing the gas pressure in a capillary leading to the valve. At the start of an experiment, helium gas was let into the capillary and liquefied by contact with the bath until the valve actuator and the lower section of the capillary were full of liquid helium. Thereafter, the valve could be opened and closed easily by changing the gas pressure in the filling line. A pressure of about 6 atm. was required to fully seal the valve. A small SA type strain gauge monitored the pressure in the actuator.

Unfortunately, the valve had a small superfluid leak. Experimentation showed that in a given run the superfluid leak rate, i.e., $-\frac{dC}{dt}$, was constant in time regardless of pressure differential across the valve. No dependence of the leak rate on temperature was observed for temperatures well below the λ line. The leakage rate changed with each opening and closing of the valve, varying from 10^{-6} pF/min to 10^{-4} pF/min. Since the leak rate was constant in time, a simple correction factor--the elapsed time multiplied by $-\frac{dC}{dt}$--could be added to each capacitance reading, thus removing the effects of the leak on the capacitance readings. Upon disassembling the valve, the problem appeared to be small flecks of solder on the valve stem. Two subsequent attempts to clean the valve to prevent leakage failed, resulting in much larger leaks.

Temperature Measurement and Regulation

The temperature of the sample chamber was measured by a calibrated Cryocal Germanium thermometer whose electrical

resistance varied from 1000 ohms at the λ line to 400,000 ohms at 0.3 K. The thermometer was tightly mounted in a copper block bolted to the sample chamber. A light coat of Apezion 'N' grease was used to provide thermal contact. The leads to the thermometer were Midohm wire whose resistance is independent of temperature. The leads were thermally anchored to the ^{4}He refrigerator, the ^{3}He refrigerator and the sample chamber by epoxying them to copper posts bolted to these objects. The resistance of the thermometer was measured on an AC resistance bridge described by Castles (1973). A Princeton Applied Research model HR 8 lock-in served as both the source of the 20 Hz driving signal and as the detector of the balance of the bridge. A G.R. standard decade resistor with a minimum resolution of 0.1 ohms was used as the known resistance in the bridge. Using this arrangement it was easy to resolve 0.02% changes in the resistance. This corresponds to a temperature resolution of better than 0.1 mK over the entire range of this experiment.

This thermometer had been calibrated against the vapor pressure of ^{3}He and ^{4}He between 0.4 K and 4.2 K by Philp (1969). He found that a form

$$T = \sum_{i=1}^{N} A_i (R^{-.518})^{i-1} \qquad (3.3)$$

where T is temperature and R is resistance with N = 5 fitted the temperature "with an RMS deviation of less than 1 mK above 0.6 K." (p. 39) A further calibration of the thermometer

against the susceptibility of CMN, extending to 0.29 K was done. These results were fitted by the same form using the program RESFIT written by Philp. These fits gave a set of coefficients, A_i, which could be substituted in Eq. (3.3) to give the temperature for any given resistance. This yielded a fit with an RMS deviation of less than 2 mK over the whole range, with a slight increase in the deviations near 0.3 K.

The out-of-balance signal of the lock-in was used to modulate the power supplied to a heater on the sample chamber. The heater was a 2000 ohm metal film resistor attached to the copper braid from the heat switch, just above the sample chamber. A metal film resistor was used because its resistance was almost independent of temperature. By suitably adjusting the bias current and the magnitude of the out-of-balance signal from the lock-in with an external circuit built for that purpose, the temperature of the sample chamber could be stabilized to within the resolution of the bridge at any temperature between 0.4 K and 1.2 K. Above 1.2 K it was necessary to reduce the cooling power of the refrigerator because the heater had insufficient power to stabilize the temperature. This could be done by pumping on the ^{3}He with only the mechanical pump, or by turning off the ^{3}He refrigerator entirely, or by turning off both the ^{3}He and ^{4}He refrigerators, depending on the temperatures required. For the very lowest temperatures, all heating and regulation were turned off and the system was allowed to slowly drift to colder temperatures. Thus regulated, the temperature was

quite stable. The largest observed drift was 4 mK over several hours.

The Sample

The sample was commercial grade helium from Air Products and Chemicals Incorporated (Airco). It was passed through a nitrogen trap with the same copper wire, molecular sieve combination as the ^{3}He return line trap previously described. The gas then passed through a trap filled with Linde #13x molecular sieve immersed in liquid helium. Testing with a Veeco MS 9 leak detector, modified to scan both the ^{3}He and ^{4}He peaks, revealed that the ^{3}He concentration was much less than 0.01%.

Procedure for Taking Data

Data were taken by recording the pressure at a fixed temperature after the system came into equilibrium. The sample was then warmed or cooled to a new temperature and another reading was taken. In most runs, the apparatus was first allowed to cool overnight. Starting from this temperature, the sample was systematically warmed in approximately 25 mK steps to some predetermined temperature greater than 1 K. Then the sample was cooled in 25 mK steps back to the original temperature. To assure consistency between runs, the same set of temperatures was used for each data pass. In the early runs that extended to the λ line, it was found that after warming to the λ line the apparatus could be cooled well below the starting temperature, but would suddenly and

irreversibly warm up to above the starting temperature. This was traced to inadequate thermal grounding of the fill capillary and valve actuator capillary. After correcting this problem, it was possible to repeatedly cover the whole P versus T curve both warming and cooling. The leakage rate through the valve was measured by holding the cell at a constant temperature for about an hour and observing the chance in capacitance. Since the P versus T curve has a maximum near 1.1 K at saturated vapor pressure and near 0.7 at 24 atm., the leakage rate was measured at this point to minimize the effect of any inaccuracies in the thermal regulation.

CHAPTER IV
RESULTS AND CONCLUSIONS

Data Reduction

The raw data consist of capacitance values versus resistance bridge readings which can be converted to pressure versus temperature. Before converting the capacitance values to pressures, two corrections to the capacitance were made. As described in Chapter III, the correction for the leakage through the valve was done by adding a constant times the elapsed time to each capacitance value. The correction is always additive because the fill capillary is evacuated to reduce the heat leak, so that the mass flow is out of the cell. By filling the capillary to a pressure greater than that of the cell, the mass flow is into the cell, the capacitance rises and the correction is subtracted from each value. In the worst case, the total leakage during a run changed the density of the liquid by less than one part in 10^4. Thus, the approximation of constant density remains valid. After applying this correction, the values of capacitance for both warming and cooling generally coincided. However, in some of the runs there were obvious discontinuities in the capacitance values, e.g., in one set of data a group of points taken while cooling the sample was exactly 4×10^{-4} pF larger than the same points taken while warming the sample. Philp had

reported "Physical shocks . . . caused the capacitance to shift discontinuously" (p. 56). The problem was eventually traced to excessively tight vibrational coupling of the cryostat to the main support frame. Small contacts with the support frame, e.g., closing the ^{3}He return line valve or bumping an exposed corner of the frame would repeatedly cause discontinuous shifts in capacitance, although moving heavy objects in the laboratory or banging the apparatus violently other than on the main frame or dewars produced no shifts in capacitance. After discovering the cause of the problem, contact with the frame was avoided. No further discontinuous shifts occurred.

Corrections for the shifts were applied in a direction which made capacitance versus temperature a smooth function. After these corrections were applied to the capacitance values, the capacitances taken when warming the sample agreed very closely with the capacitances taken when cooling the sample. In all cases the differences between warming and cooling were within three of the smallest resolved units of capacitance over the entire range from 0.4 K to 1.0 K and were frequently zero. This agreement, as well as the stability of the capacitance at a given temperature indicated that the sample was in thermal equilibrium.

The corrected capacitances were converted to pressure by Eq. (3.1), using the coefficients developed in the calibration procedure described in Chapter III. The resistances were converted to temperatures by Eq. (3.3) using the

coefficients developed in the calibration procedure described in Chapter III. From the pressure values, the density was obtained by comparing the pressure at the lowest temperature, 0.4 K, with the pressure versus density data at 0.1 K found in Table III of Abraham *et al.* (Ab, 1970). A linear interpolation was used between their data points which introduced a slight error--no more than 0.0003 gm/cm^3 for densities between 0.1451 and 0.1725 gm/cm^3--because the pressure versus density function is not strictly linear. To within the accuracy of the data of Ab (1970) 0.01 atm., the measured pressure is constant below about 0.8 K so that no significant error is introduced by using the pressure value at 0.4 K. To check this determination of density, measurements were extended to the λ line and the pressure at the λ line was compared with the measurements of pressure versus density along the λ line by Keesom and Keesom (KK, 1933). Good agreement, $\pm$ 0.0005 gm/cm^3, was found between densities determined by comparison with KK and those determined by comparison with Ab (1970), despite differences of several atmospheres in pressure between the λ line and 0.4 K for a given run. Having established this correspondence at several pressures, subsequent runs were not extended to the λ line because of experimental difficulties in doing this. For this reason, the values of density obtained from Ab (1970) were used.

Knowing the density of the sample and the temperature at each point, the roton pressure can be calculated from Eq. (2.12). Alternatively, one could have determined the roton

parameters from the data and compared these values with values determined from other experiments. This was not done for three reasons. (1) Determining the roton parameters from the data would introduce six new parameters, Δ, $\partial\Delta/\partial\rho$, μ, $\partial\mu/\partial\rho$, p_o and $\partial p_o/\partial\rho$. Four of these parameters, $\mu, \partial\mu/\partial\rho$, p_o and $\partial p_o/\partial\rho$, are difficult to measure; hence they are poorly known. (2) Such an analysis would increase the number of variables to 10 for the simplest spectrum. This is too many to be well determined from just the 20 data points in a run. (3) This would have required non-linear, least squares fitting routines which are difficult to develop and use, and can lead to spurious results.

Since $P = P_o + P_r + P_{ph}$, where P_{ph} includes both the P_{ph}', the term proportional to T^4, and the dispersion pressure, the only remaining parameter to be determined is P_o, the pressure at 0 K. Ideally, this would be determined by lowering the temperature until the pressure reaches a constant value. Since this requires a temperature of less than 0.25 K, this was impossible in this experiment. Another, less accurate, possibility is to extrapolate the lowest temperature pressures by assuming that temperature is sufficiently low that the only contribution to the pressure is the P_{ph}' which varies as T^4. This requires a substantial number of points below 0.4 K. Since heat leaks limited the experiment to T greater than 0.4 K, such a method was useless. P_o was determined from a least squares fit of $P - P_r = P_o + AT^4 + BT^6 + CT^8$. As a check on the fit, the

sound velocity was calculated from Ab (1970). The calculated value agreed closely, ± 1 to 3 m/sec out of 250 to 300 m/sec, with the experimental values given in Ab (1970). Other internal evidence, discussed later, suggests that this gave a reasonable value for P_o. The reduced data are a set of values of $P_{ph} = P - (P_o + P_r)$ versus temperature.

Because the least squares routine used will not accept more than one value of pressure for each temperature, the points taken cooling and warming were averaged together to produce a single pressure at a given temperature. The coefficients determined by the least squares fits were converted to meaningful quantities by using Eq. (2.16) with the values of C, Γ and ρ from Ab (1970) and the fundamental constants from Appendix I of Donnelly (1967).

Data Analysis

In order to display the T^4 and T^6 terms in the expression for P_{ph} as given by Eq. (2.16), a plot of P_{ph}/T^4 versus T^2 was made. Fig. 7 shows this plot for the experimental densities. If there were no dispersion, i.e., if only the phonon pressure were present, the graph would be a horizontal line. On this type of plot a T^6 dependence is a straight, non-horizontal line. The lines along the left edge of the figure indicate the position of this horizontal line for each run. The lines are labeled with the density of the sample for that run. This is a plot of the "raw" data, i.e., every observed point in this temperature range has been reduced and plotted. At higher temperatures the difference between points is smaller than the size of the symbol used to plot them. The

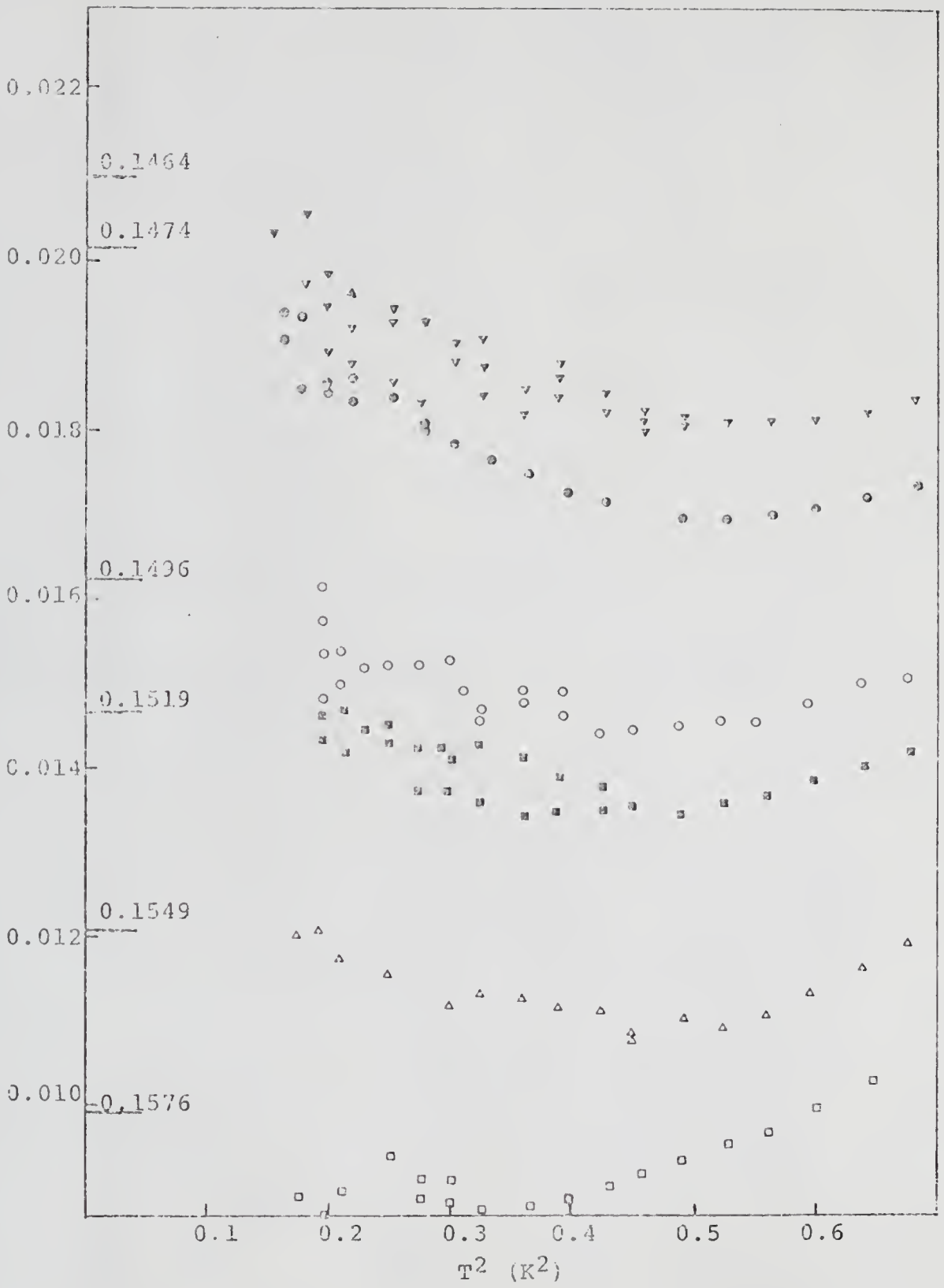

Fig. 7. P_{ph}/T^4 versus T^2. Lines indicate position of line of zero dispersion for density given on the line. Solid triangle 0.1464, solid circle 0.1474, open circle 0.1496, solid square 0.1519, open triangle 0.1549, open square 0.1576.

scatter at the lower temperatures is largely due to instrumental resolution, magnified by the T^{-4} weighting factor. The error bars represent instrumental resolution. The smoothness with which the plots approach the zero of temperature is indicative of the correctness of the method of choosing P_o. Experimentation showed that small changes in P_o produced pronounced curvature in the low temperature end of the plot--upward when P_o was too low, downward when P_o was too high. In the low temperature limit, the dispersion pressure becomes negligible so that P_{ph} is equal to P_{ph}'. Thus these plots must join the horizontal lines smoothly in the low temperature limit. The two highest densities are smooth in the low temperature limit but do not extrapolate to the phonon pressure. The reason for this is unknown.

The most noticeable and unexpected feature of these plots is the sharp upward curvature of each plot as the temperature increases. Because the curvature is upward, this represents an "excess pressure." Since the excess pressure contribution has a noticeable convex curvature, its temperature dependence is stronger than T^6. For higher densities, the magnitude of the excess pressure is larger relative to P_{ph}. Also at higher densities, the excess pressure becomes noticeable at lower temperatures. The curvature of the plots due to the excess pressure contribution is greater at higher densities than it is at lower densities.

To test whether this excess pressure arose from the T^8 term in Eq. (2.16), the points up to T = 0.85 K were fitted

with a least squares routine to the functional form $P = P_o + AT^4 + BT^6 + CT^8 + P_r$. Then, systematically the high temperature points were removed. This sharply lowered the RMS deviations, typically by a factor of five when changing from 20 to 14 points, and substantially changed, by a factor of two, the value of the coefficients B and C. Furthermore, the values of B and C for points up to 0.85 K were well outside the range of predicted values. In contrast, the values for B and C for points up to 0.7 K were in reasonable accord with predicted values. The magnitude of the excess pressure contribution substantially exceeds the value estimated for the T^8 term in Chapter II. Thus it was concluded that excess pressure was not due to the T^8 term in Eq. (2.16).

The higher order terms in Eq. (2.16) and in the expansions of other thermodynamic functions are small since these expansions are rapidly convergent with increasing powers of T, so it seems unlikely that the excess pressure arises from omitted higher order terms. While there is some evidence that the shape of the spectrum, hence γ and δ, may vary with temperature, a variation with temperature of the magnitude required to produce excess pressure seen here would totally destroy the Landau approach which is well supported by other measurements. The roton pressure could be in error, but there is no reason to believe that P_r is incorrect.

The likeliest explanation for the excess pressure is the maxons, i.e., contributions from the maximum of the excitation

spectrum which are poorly approximated by the phonon-roton model. As was argued in Chapter II, the maxon contribution to the pressure would be positive, increase with increasing density and would vary as exp (-1/T). This is consistent with the observations, since $T^4 + T^6 + T^8$ would be a poor approximation to exp (-1/T). In addition, there is evidence that a similar phenomenon was observed in the specific heat measurements. In their analysis, PWH had to limit themselves to T less than 0.7 K to achieve good fits. Furthermore, the PWH value of γ at 20 atm. is a factor of 3 higher than γ determined by neutron scattering and ultrasonic measurements, which are in good agreement with each other. PWH let the data determine the roton parameter, Δ, in contrast to this work which calculates the roton contribution to the pressure. The PWH values of Δ agree much more closely with Mills (1965) values than with Donnelly's (1972) values. As noted in Chapter II the Mills spectrum disagrees with the neutron scattering values in a fashion that would suggest an attempt to average over the maxons. The Mills spectrum is based on thermodynamic measurements. This suggests that all thermodynamic data see the effect of maxons but that these contributions are obscured by allowing the roton parameters to vary. Even with this variation of the roton parameters, the Mills spectrum remains a poor approximation to the maxons. Such an error in approximation might explain the discrepancy between γ of PWH at 20 atm. and γ from other measurements. Neutron scattering determines γ by fitting the spectrum in the small

p region. This fit is cut off below the maximum of the spectrum. Thus the maxons have no effect on the determination of γ. Ultrasonic measurements are usually taken at 0.1 K, well below the temperatures at which maxons contribute. Both the specific heat and these pressure measurements extended to 0.9 K. At that temperature, the calculation of the thermodynamic properties directly from the excitation spectrum at saturated vapor pressure by Singh (1968) showed that there were detectable discrepancies between calculations based on the phonon-roton model and direct calculations. It appears from these data that these discrepancies are larger and become detectable at lower temperatures as the density is increased.

Turning to the low temperature portion of the data, it is evident that all of the curves have an initial downward slope. This slope appears to decrease with increasing density. The coefficient of the T^6 term in Eq. (2.16) is proportional to $1/c^2$, where c is the sound velocity. Since, as the density increases, c increases, some decrease in slope of the plots in Fig. 7 would be expected. To calculate the value of $\gamma' = (\gamma - \frac{\rho}{1+5\Gamma} \frac{\partial \gamma}{\partial \rho})$ from Eq. (2.16) at different densities, the following procedure was adopted. Values of c and Γ, taken from Ab (1970) were used to calculate P_{ph}' and the constants in the coefficients of the T^6 and T^8 terms in Eq. (2.16). The quantity $P - (P_o + P_r + P_{ph}')$ was least square fitted to both a form BT^6 and a form $B'T^6 + CT^8$. Data points were systematically removed from the high temperature end until the effects

of the excess pressure were negligible. Two criteria were used to determine the absence of the excess pressure. (1) The quality of the fit from the data for the form BT^6 must not depend systematically on T. If the data used in the fit extend into the excess pressure region, the deviations increase sharply at the high temperature end. (2) The value of γ' derived from B must agree reasonably well with the value derived from B'.

The results of this procedure are shown in Table III for the four lowest densities for both the T^6 fit and the $T^6 + T^8$ fit. The three higher densities fail to join the horizontal AT^4 line smoothly at T = 0, probably due to the increasing magnitude of the excess pressure, so that fits of this type are useless. The actual numbers are accurate to only ± 10 to 25% because of the relatively small number of points fitted (10 to 15) and the sizeable changes that occur when the points are removed. Nevertheless, it is clear that γ' is negative and decreases in magnitude as the density increases. The numbers for $\delta' = 4\gamma^2 + \delta - \frac{\rho}{1+7\Gamma}\left(8\gamma \frac{\partial\gamma}{\partial\rho} + \frac{\partial\delta}{\partial\rho}\right)$ from Eq. (2.16) are about equal to $4\gamma^2 - \frac{\rho}{1+7\Gamma}\left(8\gamma \frac{\partial\gamma}{\partial\rho}\right)$, the contribution of higher powers of γ. There is very little improvement in the RMS deviations when the T^8 term is included. These values of γ' should be compared with values of γ' based on the spectra in Table I. At saturated vapor pressure, these are 8.5×10^{37} for the ultrasonic case, -2.5×10^{37} for the neutron case, and -1.26×10^{38} for the specific heat case. A plot of γ' versus density is shown in Fig. 8.

Table III. The Values of γ' and δ' at Experimental Densities.

Density in gr/cm^3	γ'^a	γ'^b	δ'^b
0.1464	-1.06×10^{38}	-1.75×10^{38}	8.75×10^{76}
0.1472	-1.19×10^{38}	-1.56×10^{38}	5.10×10^{76}
0.1496	-9.95×10^{37}	-1.95×10^{38}	9.84×10^{76}
0.1519	-5.80×10^{37}	-6.64×10^{37}	1.94×10^{76}

[a]derived from the T^6 fit

[b]derived from the $T^6 + T^8$ fit

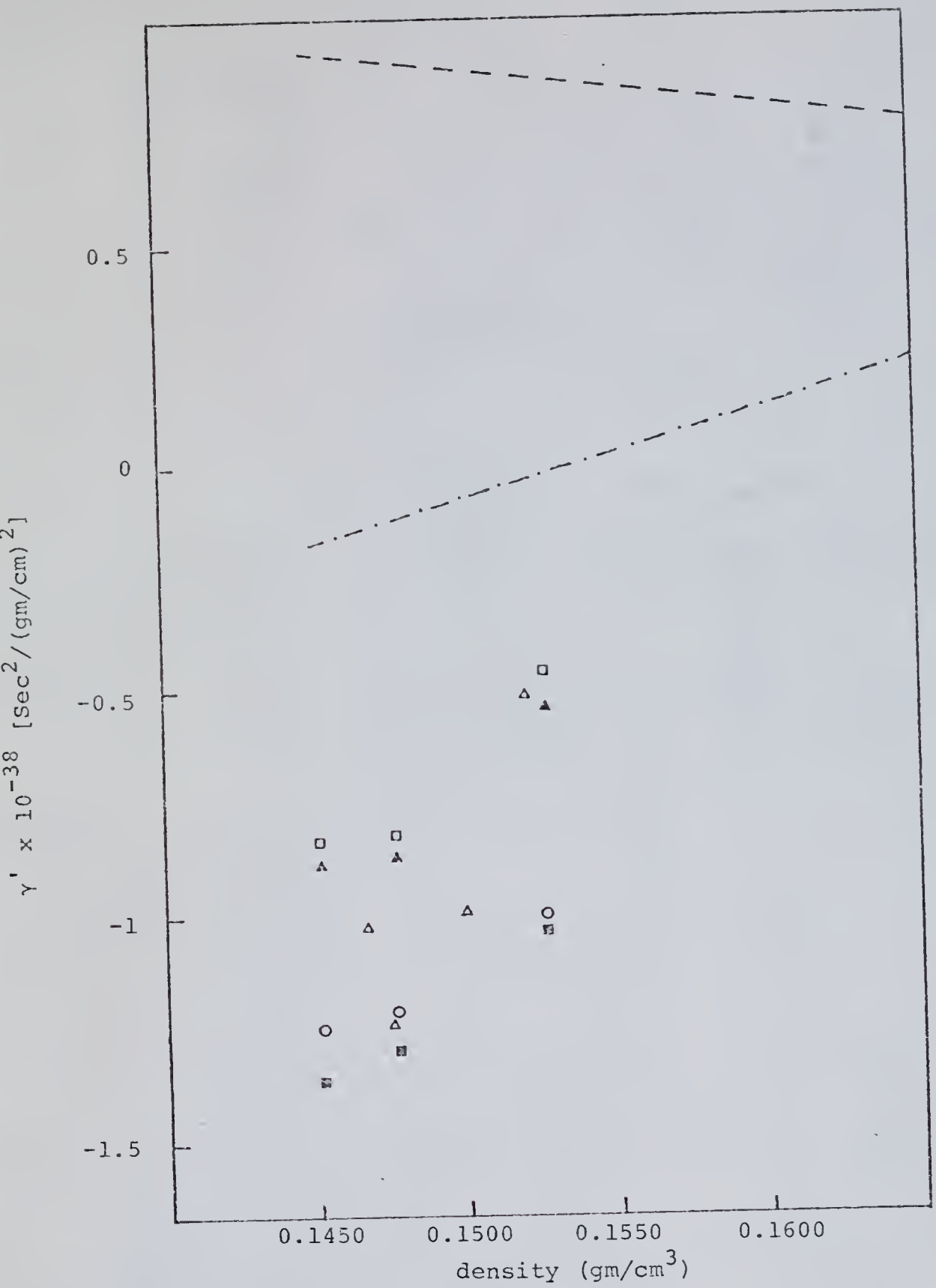

Fig. 8. γ' versus density. Open triangle this work, open square PWH assuming γ of CW at 24 atm., open circle PWH, closed triangle ZP assuming γ of CW at 24 atm., closed square ZP, dashed line is based on normal dispersion, dashed and dotted line is based on CW.

To illustrate the agreement of the pressure data with other data, Fig. 9 shows a comparison of the best data with a calculated plot for the same density, assuming γ has the PWH value as corrected by Zasada and Pathria (1974) and calculating $\frac{\partial\gamma}{\partial\rho} = (\gamma_{24\ \text{atm.}} - \gamma_{SVP})/(\rho_{24\ \text{atm.}} - \rho_{SVP})$, assuming $\gamma_{24\ \text{atm.}}$ has the CW value and γ_{SVP} has the PWH value. The data clearly follow the trend of the calculation up to the temperatures where the excess pressure becomes detectable. Further intercomparison of theories is shown in Fig. 9 by plotting γ' derived from the BT^6 fit versus density. For comparison, the values of γ' versus density for the specific heat data are shown. These are calculated using values of γ of PWH and those of PWH as corrected by Zasada and Pathria. The value of $\partial\gamma/\partial\rho$ is calculated by assuming a linear fit between the lowest and highest densities of PWH. Also shown are the values of γ' based on the ultrasonic and neutron spectra given in Table I. It is evident that there is good agreement between values of γ' derived from pressure measurements and those derived from specific heat measurements; and there is poor agreement with the neutron and ultrasonic values.

The ultimate goal of these measurements is to derive values of γ as a function of density. To do this one takes the values of γ' as a function of density and calculates γ in a self-consistent way. This is done by choosing an initial value of γ and $\partial\gamma/\partial\rho$ which yield the correct γ' at that density. These are used to calculate γ at another density, which in turn determines $\partial\gamma/\partial\rho$ at that density from γ'. These

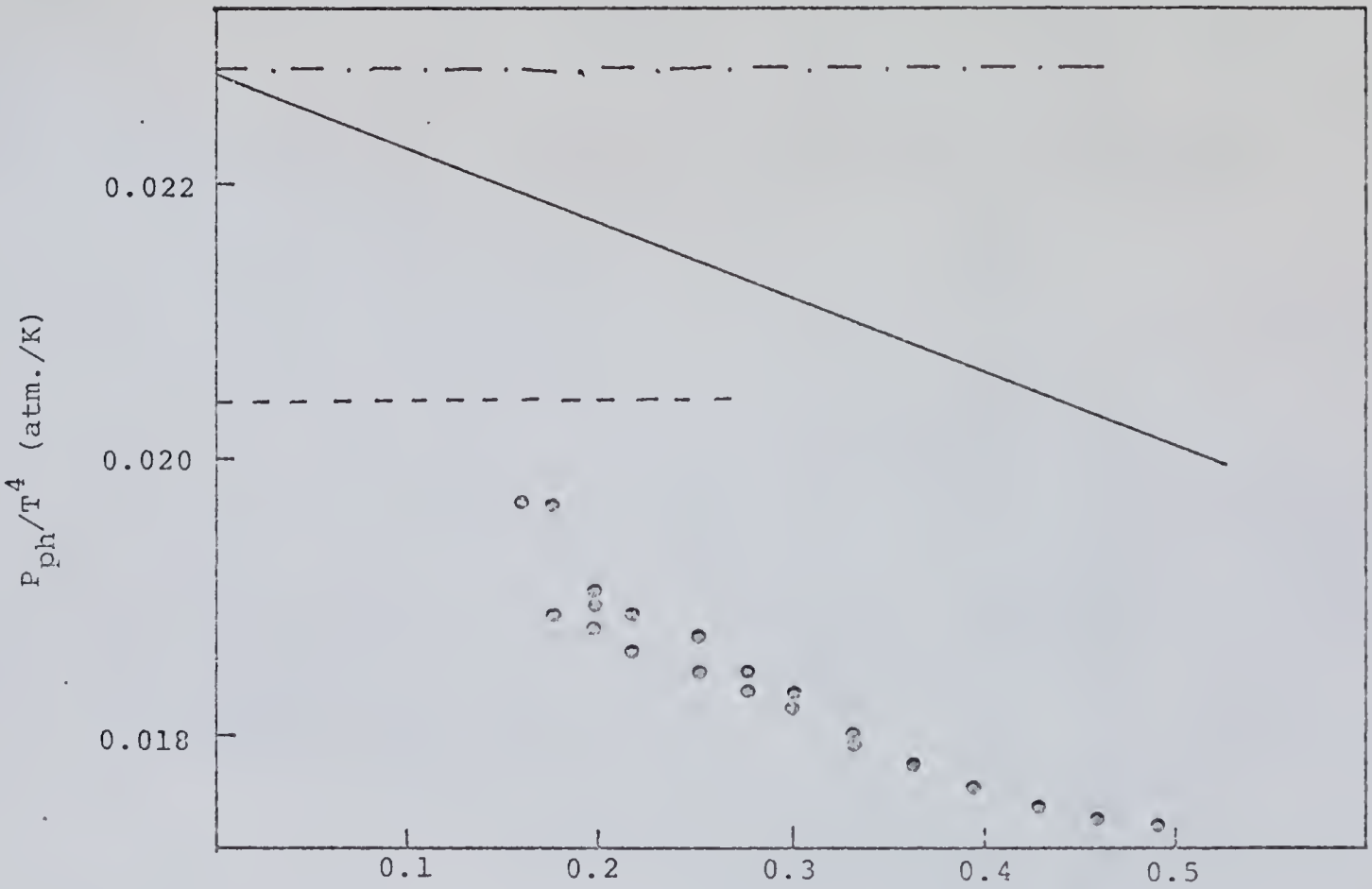

Fig. 9. P_{ph}/T^4 versus T^2 for $\rho = 0.1474$ gm/cm^3.

dashed line is the pressure with no dispersion for $\rho = 0.1474$ gm/cm^3, dashed and dotted line is the pressure with no dispersion for $\rho = 0.1451$ gm/cm^3 at SVP, solid line is the calculation at SVP for $\gamma = -5 \times 10^{37}$ and $\partial\gamma/\partial\rho = 4 \times 10^{39}$.

values are used to calculate γ and $\partial\gamma/\partial\rho$ at the next density. The process is repeated until a consistent set of γ and $\partial\gamma/\partial\rho$ are calculated, i.e., $\partial\gamma/\partial\rho$ and γ are smooth functions of density. For the present data, this is a very imprecise calculation because there are too few values of γ', the values of γ' are too uncertain and the range of densities covered is too restricted.

If the excess pressure contributions were removed, there would be a much greater range of P versus T from which to extract γ'. This would greatly improve the accuracy of γ'. Also, γ' could have been determined over a wider range of densities. Nevertheless, the fact that γ' is negative and increases with increasing density leads to the conclusion that at low pressure γ is negative and that $\partial\gamma/\partial\rho$ is positive.

The possibility of a linear dispersion term was conjectured by MR. To check this possibility, a plot for the best data of P_{ph}/T^4 versus T was made. The results are shown in Fig. 10. If P_{ph} varies at T^5 at low temperatures, the plot would be a straight line. The curvature of the plot at low temperatures is obvious. Furthermore, the curve does not extrapolate properly to T = 0. This contrasts with the linear appearance of the plot of P_{ph}/T^4 versus T^2 in Fig. 8. Thus the dispersion pressure appears to vary as T^6, rather than T^5, at low temperatures. From Eq. (2.14), this implies that $[(1+4\Gamma)(-\alpha_1)-\rho\frac{\partial\alpha_1}{\partial\rho}] = 0$. Since all of the plots in Fig. 7 appear to be similar to the best data at low temperatures, one can conclude that $\partial\alpha_1/\partial\rho = 0$ and thus $\alpha_1 = 0$. This contradicts the MR form of the dispersion curve.

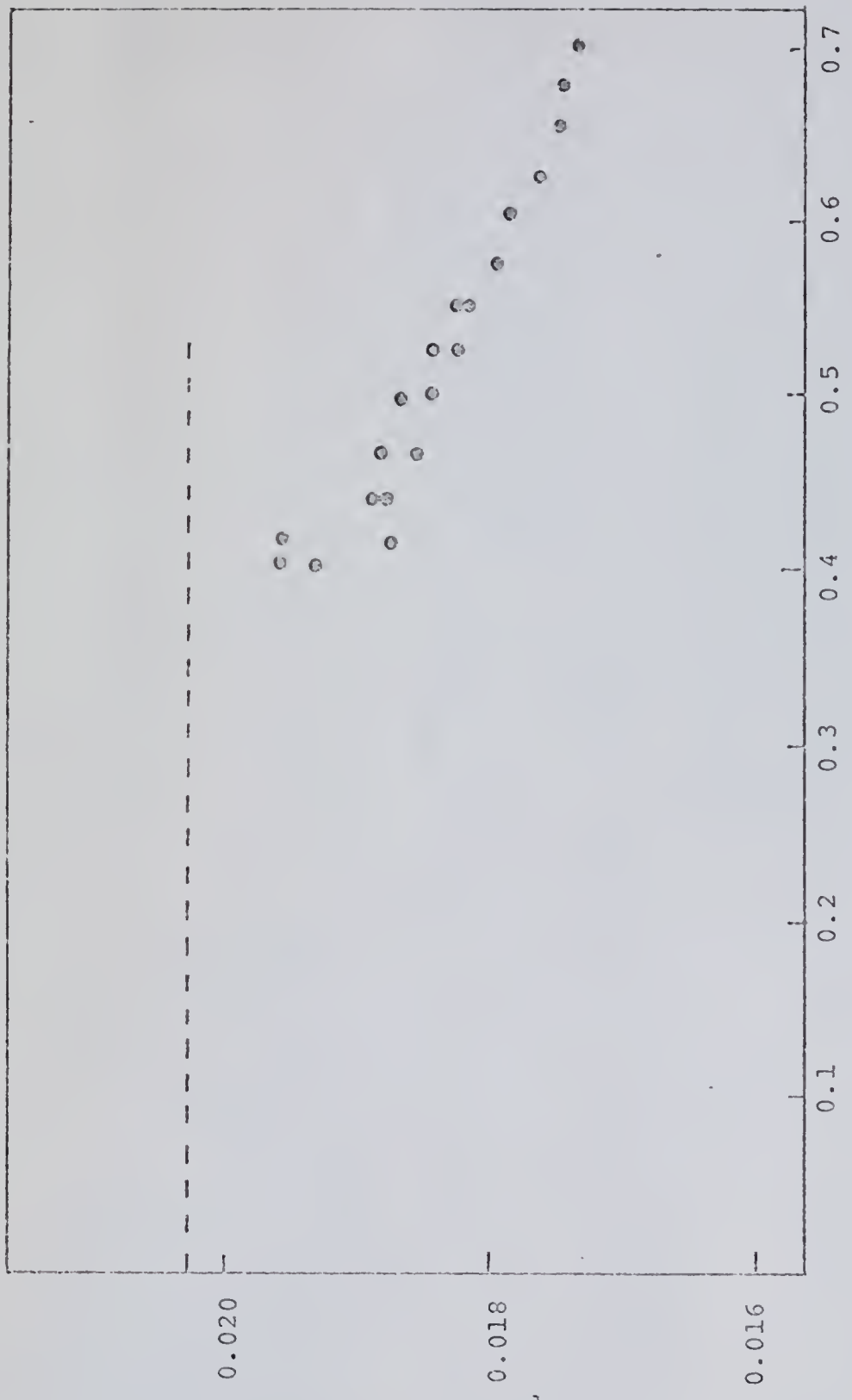

Fig. 10. P_{ph}/T^4 versus T for $\rho = 0.1474$ gm/cm^3.
dashed line is the curve for no dispersion at this density.

Conclusions

Three conclusions can be drawn from this work. (1) The MR form of the excitation spectrum is probably incorrect. (2) There is anomalous dispersion in the excitation spectrum of superfluid helium at low densities. The magnitude of the dispersion parameter and density derivative have values similar to those derived from the specific heat measurements of PWH. (3) There are contributions to the pressure other than phonons and rotons, probably maxons. These contributions increase in magnitude as the density is increased. These contributions must be removed before accurate conclusions can be made about the values of γ and $\partial\gamma/\partial\rho$ as a function of density, particularly at higher densities.

More work needs to be done in several areas before pressure measurements can be used to discriminate among the different theoretical forms for the anomalous dispersion. At present the uncertainties in this experiment are too great to permit this to be done with any confidence. The data need to be improved with more runs of the quality of the best one. The data should be extended to lower temperatures if possible to permit an unequivocal assignment of P_o based on the data. There is a need for a greater number of data points. The 25 mK spacing was used so that the change in capacitance for each change in temperature was clearly resolvable. However, an additional set of data could be taken 25 mK apart with each point being the middle of one of the present intervals. This would double the number of data points and improve the accuracy of the fits.

A method of removing the excess pressure should be devised so that the full range of temperature can be used in fitting the temperature dependence of the dispersion term. This will require an extensive neutron scattering study of the region of the maximum of the excitation curve as a function of density. Such work is in progress at the Brookhaven National Laboratory. Using those data, one could calculate the contribution due to the maxons. Such calculations could be used to reanalyze both these pressure data and the specific heat data of PWH. Such a reanalysis would improve the accuracy and the reliability of the values of γ, δ and their density derivatives.

Studies of the dispersion curve have widespread applicability, and are not just limited to studies of helium. For example, the differences among the theories largely arise from differing treatments of the interactions among excitations. Excitation models are common throughout physics, particularly in solid state physics where the concept of phonons originated. A common problem in all of these models is the treatment of the interactions of excitations. In a solid the problem is particularly complicated because of the existence of three branches of the excitation curve. Helium, a simple liquid, is a good substance for testing different theories. Thus, studies on helium could yield theories applicable to many materials.

Dispersion curves appear not only in solids but also in liquids and amorphous solids. Goda (1972) has noted that

"longitudinal phonon dispersion of some amorphous solids and simple liquids are of the phonon-roton type as observed in liquid ^{4}He. Such behavior seems to exist also in liquid metals" (p. 1064). Is the observed anomalous dispersion unique to helium, or is it a common feature of all topologically disordered substances? Perhaps precision pressure measurements of liquid neon or liquid argon could answer that question.

The universality of phonon-roton type dispersion curves suggests another reason for making detailed studies of the dispersion curve of superfluid helium. Khalatnikov (1965) gave a simple argument that claims to show that any liquid with a roton minimum will be superfluid at T = 0. That implied that the form of the dispersion curve "caused" superfluidity. The Khalatnikov argument does not predict any clearcut transition from superfluid to normal fluid as the temperature is raised unless the spectrum changes. But helium has a phonon-roton spectrum above the λ line, and is not a superfluid at that point. There are qualitative differences in the excitation spectrum of helium above and below the λ line. The line width is much broader and the temperature dependence of quantities such as the roton minimum are different. Takeno and Goda (1972) present a model which successfully predicts the spectrum of He I as well as other simple liquids but fails for He II. Accurate knowledge of the excitation spectrum for He II could lead to a better understanding of the fundamental nature of superfluidity.

This work has shown that the excitation spectrum of superfluid helium has anomalous dispersion at low densities and that for precision measurements the contributions of the maxons must be included in the theory; but it does not provide the final answer as to which theory is correct.

REFERENCES

Abraham, B. M., Y. Eckstein, J. B. Ketterson, M. Kuchnir, and J. Vignos, 1969, Phys. Rev. *181*, 347.

_____, Y. Eckstein, J. B. Ketterson, M. Kuchnir, and P. R. Roach, 1970, Phys. Rev. *A1*, 250.

Anderson. C. H., and E. S. Sabisky, 1972, Phys. Rev. Letters *28*, 80.

_____, and E. S. Sabisky, 1974, Bull. Am. Phys. Soc. *19*, 436.

Andreev, A., and I. M. Khalatnikov, 1963, Zh. Eksperim. i Teor. Fiz. *44*, 2058, [J.E.T.P. *17* (1963), 384].

Bendt, P. J., R. D. Cowan, and J. L. Yarnell, 1959, Phys. Rev. *113*, 1386.

Boghosian, C., and H. Meyer, 1966, Phys. Rev. *152*, 200.

Castles, S. H., 1973, Ph.D. Dissertation, University of Florida.

Cowley, R. A., and A. D. B. Woods, 1971, Can. J. Phys. *49*, 177.

Dietrich, O. W., E. H. Graf, C. H. Huang, and L. Passell, 1972, Phys. Rev. *A5*, 1377.

Donnelly, R. J., 1967, *Experimental Superfluidity* (University of Chicago Press, Chicago).

_____, 1972, Phys. Letters *39A*, 221.

Dynes, R. C., and V. Narayanamurti, 1974, Bull. Am. Phys. Soc. *19*, 435.

Eckstein, S., and B. B. Varga, 1968, Phys. Rev. Letters *21*, 1311.

Feenberg, E., 1971, Phys. Rev. Letters *26*, 301.

Feynman, R. P., 1953, Phys. Rev. *91*, 1301.

_____, 1954, in *Progress in Low Temperature Physics*, Volume I, edited by C. J. Gorter (Interscience Publishers, New York).

_____, 1954b, Phys. Rev. *94*, 262.

_____, and M. Cohen, 1956, Phys. Rev. *102*, 1189.

_____, and M. Cohen, 1957, Phys. Rev. *107*, 13.

Friedlander, D. R., S. G. Eckstein, and C. G. Kuyper, 1972, Phys. Rev. Letters *30*, 78.

Goda, M., 1972, Prog. Theor. Phys. *47*, 1064.

Gould, H., and V. K. Wong, 1971, Phys. Rev. Letters *27*, 301.

Hallock, R. B., 1972, Phys. Rev. *A5*, 320.

Havlin, S., and M. Luban, 1972, Phys. Letters *42A*, 133.

Heberlein, D. C., 1969, Ph.D. Dissertation, University of Florida.

Henshaw, D. G., and A. D. B. Woods, 1961, Phys. Rev. *121*, 1266.

Iachello, F., and M. Rassetti, 1973, Lettere al Nuovo Cim. *7*, 295.

Ishikawa, K., and K. Yamada, 1972, Prog. Theor. Phys. *47*, 1455.

Jackle, J., and K. W. Kehr, 1971, Phys. Rev. Letters *27*, 654.

_____, and K. W. Kehr, 1974, Phys. Rev. *A9*, 1757.

Jackson, H. W., 1974, Phys. Rev. *A10*, 278.

Kammerlingh Onnes, H., 1908, Leiden Communication *108*.

Keesom, W. H., and A. H. Keesom, 1933, Leiden Communication *224d*.

Keller, W. E., 1969, *Helium-3 and Helium-4* (Plenum Press, New York).

Khalatnikov, I. M., 1965, *Introduction to the Theory of Superfluidity* (Benjamin, New York).

_____, and D. M. Chernikova, 1965, Zh. Eksperim. i Teor. Fiz. *49*, 1957, [J.E.T.P. *22* (1966), 1336].

_____, and D. M. Chernikova, 1966, Zh. Eksperim. i Teor. Fiz. *50*, 411, [J.E.T.P. *23* (1966), 274].

Kirk, W. P., S. H. Castles, and E. D. Adams, 1971, Rev. Sci. Instr. *41*, 1007.

Landau, L. D., 1941, Zh. Eksperim. i Teor. Fiz. *5*, 71, translated in I. M. Khalatnikov, 1965, *Introduction to Superfluidity* (Benjamin, New York).

_____, 1947, Zh. Eksperim. i Teor. Fiz. *11*, 91, translated in I. M. Khalatnikov, 1965, *Introduction to Superfluidity* (Benjamin, New York).

London, F., 1954, *Superfluids Volume II: Macroscopic Theory of Superfluid Helium* (Dover Publications Inc., New York).

Lin-Liu, Yu-Reh, and Chia-Wei Woo, 1974, J. Low Temp. Phys. *14*, 317.

Maris, H. J., 1972, Phys. Rev. Letters *28*, 277.

_____, 1973, Phys. Rev. *A8*, 2629.

_____, and W. F. Massey, 1970, Phys. Rev. Letters *25*, 220.

Mills, R. L., 1965, Ann. Phys. (New York) *35*, 410.

Mills, N. G., R. A. Sherlock, and A. F. G. Wyatt, 1974, Phys. Rev. Letters *32*, 978.

Molinari, A., and T. Regge, 1971, Phys. Rev. Letters *26*, 1531.

Narayanamurti, V., K. Andres, and R. C. Dynes, 1973, Phys. Rev. Letters *31*, 687.

Petick, C. J., and D. Ter Haar, 1966, Physica *32*, 1905.

Phillips, N. E., C. G. Waterfield and J. K. Hoffer, 1970, Phys. Rev. Letters *25*, 1260.

Philp, J. W., 1969, Ph.D. Dissertation, University of Florida.

Pokrant, M. A., 1972, Phys. Rev. *A6*, 1588.

Roach, P. R., J. B. Ketterson, and M. Kuchnir, 1972a, Phys. Rev. *A5*, 2205.

_____, J. B. Ketterson, M. Kuchnir, and B. M. Abraham, 1972b, J. Low Temp. Phys. *9*, 105.

_____, B. M. Abraham, J. B. Ketterson, and M. Kuchnir, 1972c, Phys. Rev. Letters *29*, 32.

_____, J. B. Ketterson, and M. Kuchnir, 1972d, Rev. Sci. Instr. *43*, 898.

_____, J. B. Ketterson, B. M. Abraham, and M. Kuchnir, 1972e, Phys. Letters *39A*, 251.

Simon, S., 1963, Proc. Phys. Soc. (London) *82*, 401.

Singh, A. D., 1968, Can. J. Phys. *46*, 1801.

Straty, G. C., and E. D. Adams, 1969, Rev. Sci. Instr. *40*, 1393.

Svensson, E. C., A. D. B. Woods, and P. Martel, 1972, Phys. Rev. Letters *29*, 1148.

Takeno, S., and M. Goda, 1972, Prog. Theo. Phys. *48*, 724.

van den Meijdenberg, C. J., K. W. Taconis, and R. de Bruyn Ouboter, 1961, Physica *27*, 197.

Walsh, P. J., 1963, M.S. Thesis, University of Florida.

Wilks, J., 1967, *Properties of Liquid and Solid Helium* (Clarendon Press, Oxford, England).

Woods, A. D. B., and R. A. Cowley, 1973, Reports Prog. Phys. *36*, 1135.

Yarnell, J. L., G. P. Arnold, P. J. Bendt, and E. C. Kerr, 1959, Phys. Rev. *113*, 1379.

Zasada, C., and R. K. Pathria, 1972, Phys. Rev. Letters *29*, 988.

_____, and R. K. Pathria, 1974, Phys. Rev. *A9*, 560.

BIOGRAPHICAL SKETCH

Albert Robert Menard III was born July 17, 1943 at Boston, Massachusetts. A National Merit Scholarship finalist, he graduated from Boulder High School in Boulder, Colorado in June, 1961. In June, 1965, he received the Bachelor of Arts degree from Amherst College, Amherst, Massachusetts. He then enrolled in the Graduate School of the University of Minnesota, where he received the degree of Master of Science in March, 1969.

In September, 1969, he enrolled in the Graduate School of the University of Florida to pursue the degree of Doctor of Philosophy. From January through August, 1973, he was a National Science Foundation trainee.

Mr. Menard is a member of Sigma Pi Sigma and the American Physical Society.

He is married to the former Anne Elaine Dozer of Greencastle, Indiana. They have one daughter, Laura Elizabeth, born in June, 1972.

I certify that I have read this study and that in my opinion it conforms to acceptable standards of scholarly presentation and is fully adequate, in scope and quality, as a dissertation for the degree of Doctor of Philosophy.

E. Dwight Adams

E. Dwight Adams, Chairman
Professor of Physics

I certify that I have read this study and that in my opinion it conforms to acceptable standards of scholarly presentation and is fully adequate, in scope and quality, as a dissertation for the degree of Doctor of Philosophy.

Arthur A. Broyles

Arthur A. Broyles
Professor of Physics and Astronomy

I certify that I have read this study and that in my opinion it conforms to acceptable standards of scholarly presentation and is fully adequate, in scope and quality, as a dissertation for the degree of Doctor of Philosophy.

Thomas L. Bailey

Thomas L. Bailey
Professor of Physics

I certify that I have read this study and that in my opinion it conforms to acceptable standards of scholarly presentation and is fully adequate, in scope and quality, as a dissertation for the degree of Doctor of Philosophy.

Wiley P. Kirk

Wiley P. Kirk
Assistant Professor of Physics

I certify that I have read this study and that in my opinion it conforms to acceptable standards of scholarly presentation and is fully adequate, in scope and quality, as a dissertation for the degree of Doctor of Philosophy.

Arun Kumar Varma

Arun K. Varma
Associate Professor of Mathematics

This thesis was submitted to the Graduate Faculty of the Department of Physics in the College of Arts and Sciences and to the Graduate Council, and was accepted as partial fulfillment of the requirements for the degree of Doctor of Philosophy.

December, 1974

Dean, Graduate School